Axon generation and myelination in motor neuron-Schwann cell coculture model

Sujin Hyung

Department of Medical Science

The Graduate School, Yonsei University

연세대학교
YONSEI UNIVERSITY

Axon generation and myelination in motor neuron-Schwann cell coculture model

Directed by Professor Jong-Chul Park

The Doctoral Dissertation
submitted to the Department of Medical Science
the Graduate School of Yonsei University
in partial fulfillment of the requirements for the
degree of Doctor of Philosophy

Sujin Hyung

December 2016

This certifies that the Doctoral Dissertation
of Sujin Hyung is approved.

_____

Thesis supervisor: Jong-Chul Park

_____

Thesis Committee Member: Jun-Kyo Francis Suh

_____

Thesis Committee Member: Chul Hoon Kim

_____

Thesis Committee Member: Noo Li Jeon

_____

Thesis Committee Member: Hosung Jung

The Graduate School

Yonsei University

December 2016

Acknowledgements

5 년의 시간 동안 많은 것을 배운 것 같습니다. 무엇보다도 박사학위 동안 연구 자체에 대한 열정을 잃지 않도록 해주신 주님께 감사드립니다. 실패에 좌절하는 저를 다시 일으켜 주시고 항상 겸손하는 마음을 잃지 않도록 지지해 주셔서 감사합니다.

연세대학교와 한국 과학 기술 연구원의 학연생으로서 남들과는 조금은 다른 좀 더 폭넓은 학위 생활을 했던 것 같습니다. 좋은 연구주제를 가지고 자유롭게 연구에만 몰입할 수 있게 든든한 지도를 해주신 박종철 교수님, 서준교 박사님 진심으로 감사합니다. 찾아 뵐 때마다 항상 따뜻하게 저의 이야기를 들어 주시고 조언해 주신 박종철 교수님 덕분에 마음의 용기를 얻었습니다. 그리고 항상 꼼꼼하게 지도 뿐 만 아니라 좋은 연구자가 될 수 있도록 기회를 열어주신 서준교 박사님, 저에게 박사님의 마지막 제자가 될 영광을 주셔서 진심으로 감사합니다.

학위를 하는 동안 많은 깨우침을 주신 훌륭하신 분들을 많이 만났습니다. 먼저 저의 심사위원이신 김철훈 교수님, 정호성 교수님 좋은 조언을 해주셔서 감사합니다. 항상 친절하게 다양한 분야의 연구 영역에 접근할 수 있도록 기회를 주신 전누리 교수님, 그리고 연구라는 열정을 다시 한 번 새롭게 느끼게 해주신 허은미 박사님, 지금도 항상 많은 것을 배웁니다. 감사합니다. 바이오닉스 연구단에 있는 동안 좋은 인격을 지니신 박사님을 많이 만났습니다. 뒤에서 따뜻하게 저의 연구를 지지해 주셨던 김진석 박사님, 졸업을 앞 둔 지금 저의 기억에 자리 잡은 좋은 박사님 이십니다. 묵묵히 저를 응원해 주신 신현준 박사님, 윤인찬 박사님께도 진심으로 감사합니다.

바이오닉스 연구단은 인격이 훌륭하신 박사님들 뿐 만 아니라 이를 따르는 좋은 학생들도 많았습니다. 우선 열정 가득한 성희씨, 강일오빠 지금처럼 열정 가득한 모습으로 나중에 같이 연구할 수 있는 날을 기다려봅니다. 그리고 키스트에서 휴식처 같은 동휘오빠, 많은 이야기를 나누진 못했지만 인사만으로도 공감할 수 있었던 민경씨 앞으로 좋은 연구 하셔서 뜻깊은 마무리 하시길 바랍니다.

이 뿐만 아니라 동훈씨, 헌휘씨, 진기, 병성이에게도 감사함을 표합니다.
그리고 자주 만나지 못하지만 만날 때마다 항상 반겨주는 학교동료인 민성오빠, 병주, 민아, 경미, 혜진, 그리고 항상 좋은 조언을 해주신 미희 언니 감사합니다.

저의 연구는 이 분들이 없었다면 결코 완성할 수 없었습니다. 처음 연구의 시작을 함께 했던 나라, 짧은 시간이지만 함께 했던 자윤, 인생의 즐거움까지 느끼게 해준 라마와 가비, 그리고 마지막까지 함께 해준 연지에게 깊은 감사함을 전합니다. 바쁜 실험 일정도 묵묵히 견뎌내고 실패에 빠졌을 때 저에게 새로운 시각으로 연구를 접근할 수 있도록 해준 동료 덕분에 용기를 잃지 않았습니다.

그리고 보윤 선생님, 키스트에서 좋은 벗을 만났습니다. 감사합니다.

무엇보다도 좋은 연구를 할 수 있었던 것은 저를 정신적으로 지지해준 사람이 있어서 가능 하였습니다. 항상 기도로 지지하고 응원해준 은숙 이모, 앞으로도 겸손함 잃지 않겠습니다. 묵묵히 저의 이야기를 들어주고 용기를 준 환이에게도 감사함을 전합니다. 마지막으로 언제나 저를 지지해 주는 가족..힘들 때 마다 누구보다 같이 걱정해 주고 가장 먼저 기뻐해 주는 가족이 있어서 저는 학위에 몰두할 수 있었습니다. 특히 석사과정부터 박사과정까지 오랜 기간 동안 저를 지켜주신 아버지 형만욱님과 어머니 정송자님, 진심으로 감사하고 그리고 사랑합니다.

TABLE OF CONTENTS

Abstract 1

Chapter I. Introduction

1. Research Background 4
2. Outline of Dissertation 17

Chapter II. 2-D Coculture of Primary Motor Neurons and Schwann Cells

1. Introduction 19
2. Materials and Methods 21
3. Results 35

Chapter III. Progranulin (PGRN), A Novel SC-Secreting Protein: Effects on Viability and Axon Growth of Motor Neuron

1. Introduction 50
2. Materials and Methods 52
3. Results 55

Chapter IV. Optogenetic Stimulation of Axon Growth of Motor Neuron

1. Introduction 68
2. Materials and Methods 70

3. Results 75

Chapter V. 3-D Coculture Model of MN-SC in Microfluidic Biochip

1. Introduction 83
2. Materials and Methods 85
3. Results 88

Chapter VI. Discussion and Conclusion

1. Discussion 100
2. Conclusion 109

References 110

Abstract (In Korean) 128

LIST OF FIGRES

Chapter I.

Figure 1.1. Schematic comparison of myelin formation in CNS and PNS neurons 5
Figure 1.2. Microfluidic biochips to study development of nervous system 9
Figure 1.3. Overview of PGRN structure and granulination process 12
Figure 1.4. Schematic drawing summarizing the actions of axon growth by optogenetic stimulation 14
Figure 1.5. Overview of the dissertation. We established MN-SC coculture model for generation and myelination of axon from 2-D to 3-D culture using microfluidic biochip 16

Chapter II.

Figure 2.1. Identification of purified SCs monoculture by confocal microscopy 25

Figure 2.2. Identification of purified MNs monoculture by confocal microscopy 28
Figure 2.3. Schematic illustration of MN monoculture and MN-SC coculture on a Matrigel 36
Figure 2.4. Flowchart of differentiation of MNs in culture 37
Figure 2.5. Cell viability in MN monoculture and MN-SC coculture 39
Figure 2.6. Axonal outgrowth in MN monoculture and MN-SC coculture 41
Figure 2.7. Differentiation of neurons and SCs in MN-SC coculture 43
Figure 2.8. Increased expression of Krox20 and MBP protein in MN-SCs coculture 44
Figure 2.9. Formation of compact myelin sheaths in the MN-SCs coculture model 44
Figure 2.10. Myelination of axons in the MN-SC coculture model 45
Figure 2.11. Pre-myelinating and myelinating SCs 47
Figure 2.12. Effects of drug treatment on myelination 49

Chapter III.

Figure 3.1. Cell viability was examined between MN monoculture and MN-SC coculture using transwell 56
Figure 3.2. Identification of PGRN secretion in SCs conditioned medium using Liquid Chromatography-Tandem Mass Spectrometry 59
Figure 3.3. Increase in PGRN secretion by day-dependent SCs 61
Figure 3.4. Increased expression of PGRN by serum levels-dependent SCs.....62
Figure 3.5. Axon growth of MN was dependent on the concentrations of PGRN and SLPI, a molecule which deactivates PGRN by blocking the hydrolysis of the protein 64
Figure 3.6. Protection of PGRN fragments against MNs' cell death.....67
Figure 3.7. Promotion of axon growth of MNs by PGRN fragments..... 67

Chapter IV.

Figure 4.1. Gene map of pAAV-CMV-CatCh-EYFP 71
Figure 4.2. The schematic depiction of a custom LED array for optical stimulation.....73
Figure 4.3. CatCh-expression in MNs 76
Figure 4.4. Cell viability by optical stimulation at different intensities.....78
Figure 4.5. Axon growth of CatCh-MN by optogenetic stimulation.....80
Figure 4.6. Intracellular level of cAMP (B) and PKA (C) expression in 2-D MN culture under optogenetic stimulation.....82

Chapter V.

Figure 5.1. 3-D MN-SC coculture model on microfluidic biochip..... 90
Figure 5.2. Temporal flowchart describing the protocols of 3-D MN-SC coculture study 92

Figure 5.3. Axon growth of MN monoculture in 3-D microfluidic biochip with or without optical stimulation 94
Figure 5.4. Effects of optogenetic stimulation and/or Co-Q10 treatment on axon growth of MN in 3-D MN-SC coculture model.....95
Figure 5.5. Effects of optogenetic stimulation and/or Co-Q10 treatment on MBP expression of MN in 3-D MN-SC coculture model.....98
Figure 5.6. Representative 3-D reconstruction image of MN-SC coculture on the biochip 99

LIST OF TABLES

Table 1. Composition of SC basic medium 23

Table 2. Composition of SC growth medium 23

Table 3. Complement-mediated cytolysis 24

Table 4. Composition of MN medium 27

Table 5. Depolarization solution 27

Table 6. Composition of MN-SC medium 30

Abstract

Axon generation and myelination in motor neuron-Schwann cell coculture model

Sujin Hyung

Department of Medical Science

The Graduate School, Yonsei University

(Directed by Professor Jong-Chul Park)

Myelination in the nervous system is an important structural element to electrically insulate the axon for the propagation of action potential with increased conduction velocity. In the peripheral nervous system (PNS), each Schwann cell corresponds with one internode in myelin sheath that is essential for the maintenance of propriety and functions of peripheral nerves. However, the deficiency of peripheral nerves in both disease and

injury model still remains unsolved and studies to recover this limitation have been performed *in vivo* as well as *in vitro*. Here, we successfully constructed 2-D and 3-D models of the motor nervous system. We first constructed 2-D MN-SC coculture on coverslip to understand interactions between MNs and SCs, and then developed 3-D MN-SC coculture model on the microfluidic biochips to recapitulate *in vivo* conditions. MN is reportedly difficult to culture for more than a week. However, MNs were well-maintained in our coculture model for more than a mo. During this time, SCs not only supported the survival of motor neuron but also promoted the outgrowth of axons. This effect was found to arise from the SC-secreted progranulin (PGRN) and the secretion of this protein was regulated by SC proliferation. We found that PGRN and their fragments, GRN C and GRN E, function as strong neurotrophic factors, enabling the viability of MNs for more than two weeks in MN culture without SCs. Furthermore, we found that the axon outgrowth could be promoted by optogenetic stimulation with a dramatic effect in MN monocultures. Furthermore, SC is a structurally important cell source, which forms myelin. We performed temporal quantitative measurement of SC in the coculture model and found the effect of coenzyme Q10 on the myelination promotion. These findings provide a very useful tool to enable us to break through the limitations in motor nervous system research. Our results might help to decipher the

myelination mechanism and learn more about MN diseases such as ALS, through drug screening. Furthermore, this *in vivo* mimicking *in vitro* model, might help in the study of post-injury mechanisms in greater detail by overcoming the limitations in the field of regeneration.

Key Words: Motor neuron, Schwann cell, axon growth, myelination, progranulin, optogenetic stimulation, 3-dimensional microfluidic biochip

Chapter I.

Introduction

1. Research Background

Myelin provides an electrically insulating material that forms a multilayered sheath around the axon of a neuron. In the peripheral nervous system (PNS), myelin sheath is generated by Schwann cells (SCs), whereas in the central nervous system (CNS), myelin is produced by oligodendrocytes (Fig. 1.1). The myelin sheath of axons formed by SCs and oligodendrocytes not only facilitates the conduction of action potentials in the nervous system, but also protects axons and provides nutritional support to the associated axons. Various defects in myelination, such as hypomyelination, delayed myelination, or demyelination, are known to cause debilitating neurological disorders.[1-4] Hence, understanding how SCs and oligodendrocytes not only produce

myelin during developmental process and remyelinate axons during repair process of damaged neurons, is of enormous scientific interest. In many cases of nerve repair after physical injury, an incomplete myelination of regenerated nerve fibers often results in malfunction of the repaired nerve.[5]

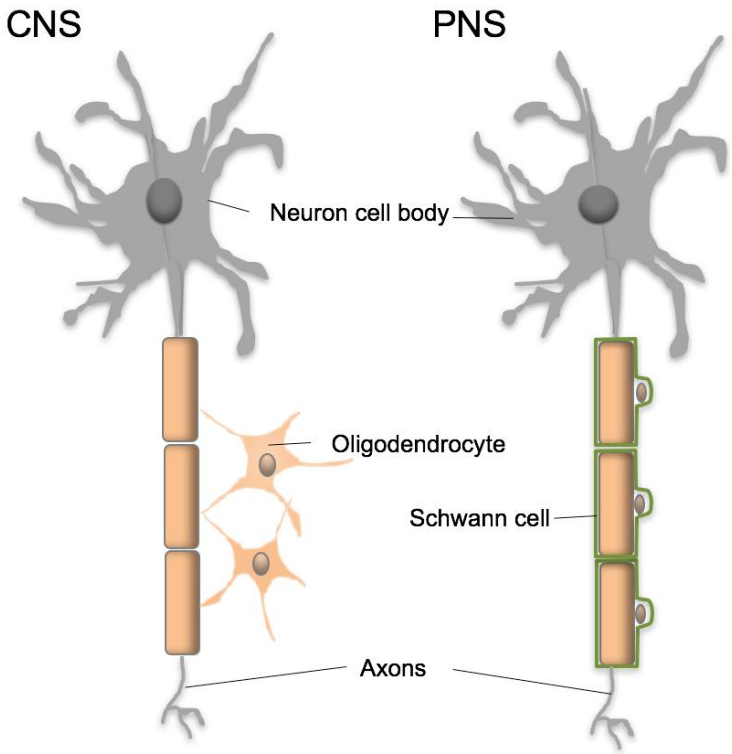

Figure 1.1. Schematic comparison of myelin formation in CNS and PNS neurons. In the CNS, a single oligodendrocyte controls multiple neurons while in the PNS a single SC forms myelin around a part of a single neuron as glial cell.

Several *in vivo* animal studies have been conducted to resolve the issue of limited neuronal repair process. The use of autologous[6-8] or artificial nerve grafts[9-11] has been reported to allow the repair of nerve defects when the injury gap is small or large. However, this repair process is associated with donor site morbidity as well as inadequate functional reinnervation causing inflammation. The reconstitution of the myelin sheath is eventually hard to achieve in such cases.

Several *in vitro* models have also been developed. Methods to culture SCs and oligodendrocytes have been established and extensively applied to investigate the biology of myelinating glia.[12-14] These cultures greatly improved the understanding of how SCs and oligodendrocytes differentiate and mature. In addition to culture systems comprising pure SCs or oligodendrocytes, a coculture system composed of both neurons and myelinating glia can provide insights into the interactions between myelinating glial cells and axons as well as the myelination process. Various coculture systems have been reported in literature, such as coculture of oligodendrocytes and hippocampal neurons,[14] SCs and sensory neurons (from dorsal root ganglia),[12] and oligodendrocytes and retinal ganglion cells.[15] Recently, Gingras *et al.*[16] reported a method of culturing primary MNs on collagen-chitosan sponges seeded with fibroblasts or with a mixture of fibroblasts and SCs. While the coculture model of Gingras *et al.*[16] enabled a long-term culture (lasting more than a

mo) of MN, the protocol required 21 days of a pre−culture for fibroblasts and/or SCs before the addition of MNs. They also reported that increased axon outgrowth could be achieved by several exogenous neurotrophic supplements, such as BDNF, neurotrophin-3, glial-derived neurotrophic factor, and ciliary neurotrophic factor. On the other hand, Haastert *et al.*[17] reported that when cultured on a feeder layer of SCs, MNs survived in culture without supplementary support of neurotrophic factors for 20 days *in vitro* (DIV), but the viability of MNs gradually reduced from more than 70% on DIV 3 to 12% by DIV 20. In addition, in the coculture model of MNs and SCs, mature MNs had enlarged somata but myelination of MN axons by SCs was not achieved during the culture period.

A few studies have used the *in vitro* culture method to recapitulate the nervous system on microfluidic biochips, based on microfabrication technologies.[14,18-22] These techniques enable the development of elaborate devices to manipulate neurons and can be used to construct the microscopic structure in biocompatible materials such as polydimethysiloxane (PDMS). Taylor *et al.*[14] reported a method for culturing hippocampal neurons and oligodendrocytes using microfluidic platform, which enabled *in vitro* model that mimicked *in vivo* conditions for separating cell bodies and axon of neurons. These 2-D coculture

models provide insights into environment condition of neuron-glia interaction and myelin process, and eventually manipulation of these cells. Furthermore, Park *et. al.*[21] reported a novel platform composed of multi-compartment chambers, which enable isolation of axons from cell bodies and can be used for screening drugs as well as molecular factors that activate axon growth (Fig. 1.2). There is a substantial research interest in studying both physical interaction and molecular signals of neuron-glia during the development of nervous system to elucidate how to facilitate successful nerve repair after nerve damage as well as maintain healthy neurons through special stimulatory factor and/ or neurotrophic factors.

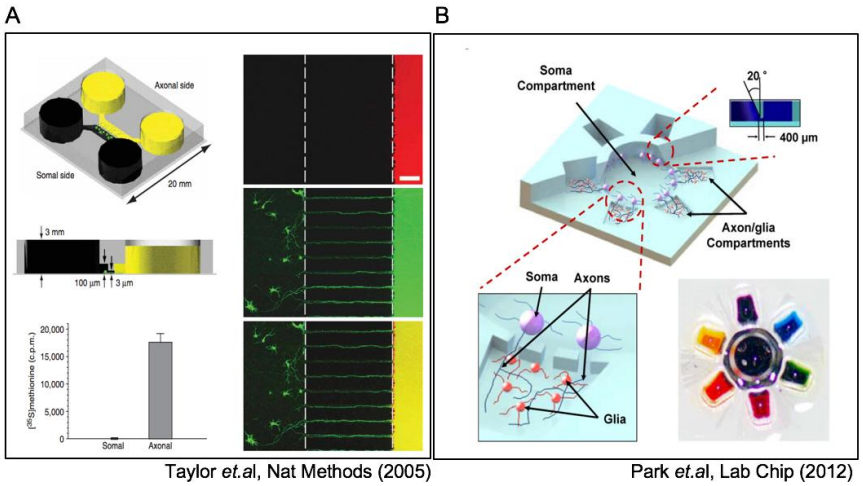

Figure 1.2. Microfluidic biochips to study development of nervous system. (A) The biochip induces axon growth of CNS neurons and isolates axons that were generated fluidically by volume difference between two chambers (images reproduced from Taylor *et al.* 2005). (B) The biochip consists of six axon-glia compartments that enabled carrying out multiple biomolecular treatment in 2-D neuron-glia coculture model (images reproduced from Park *et al.* 2012).

Previous studies reported that axon growth and viability of neurons significantly increased when cultured with supplementary support of exogenous neurotrophic factors including brain-derived neurotrophic factor (BDNF),[23] nerve growth factor (NGF),[24] glia-derived neurotrophic factor (GDNF),[25] ciliary neurotrophic factor (CNTF).[26] Furthermore, insulin–like growth factor-1 (IGF-1), functioning as a neurotrophic factor,

enabled promotion of axon outgrowth of MNs[27] and regulated the establishment of hippocampal neuronal polarity through the IGF-1 receptor.[28] Furthermore, these neurotrophic factors have a critical role in both neurodegenerative and metabolic diseases.

In particular, recent studies investigated progranulin (PGRN), also known as proepithelin, granulin-epithelin precursor or PC cell-derived growth factor, composed of 7.5 granulins (Fig. 1.3, top panel), and is a key regulator in a subset of frontotemporal dementias (FTLD), which is one of the most common neurodegenerative disease resulting in behavior and/or speech changes.[29,30] Pathogenic loss-of function of PGRN causes FTLD characterized by progressive deterioration of frontotemporal lobes and might induce susceptibility to metabolic disease.[31] However, it is unclear how variation in PGRN causes these diverse diseases and more studies are required to clarify the mechanism that mediate PGRN function. PGRN is widely expressed in many cell types, including immune cells, adipocytes, epithelial cells, and neurons in the CNS and PNS, and participates in wound repair,[32] inflammation to tumor growth,[33] and neurodevelopment.[29] In particular, PGRN plays a dual role in wound response wherein mRNA expression of PGRN was upregulated by specific cell types, including macrophages, neutrophils, enthothelia cells, and fibroblast after wounding, but diminished in intact skin. PGRN expression at injury site induces accumulation of immune cells,

fibroblast, and blood vessels to promote cell division, migration, and formulation of and tubule-like structure.[32] Therefore, PGRN might play a critical role in growth factor in wound healing.[32] (Fig. 1.3, bottom panel) Recently, PGRN has emerged as a novel angiogenic growth factor, derived from human mesothelioma cells, which might promote cell proliferation and survival by activating proteins and induce VEGF-independent angiogenesis.[33] In addition, a few studies reported that PGRN enhances neurite outgrowth in cortical and hippocampal neurons[31] as well as axon branching of hippocampal neurons,[34] supporting the role of PGRN as a neurotrophic factor.[35] Taken together, PGRN might play a key role in repair process after injury, wherein PGRN expression is dramatically upregulated in immune cells and cleaved into granulins by proteases as previously described.[29,32]

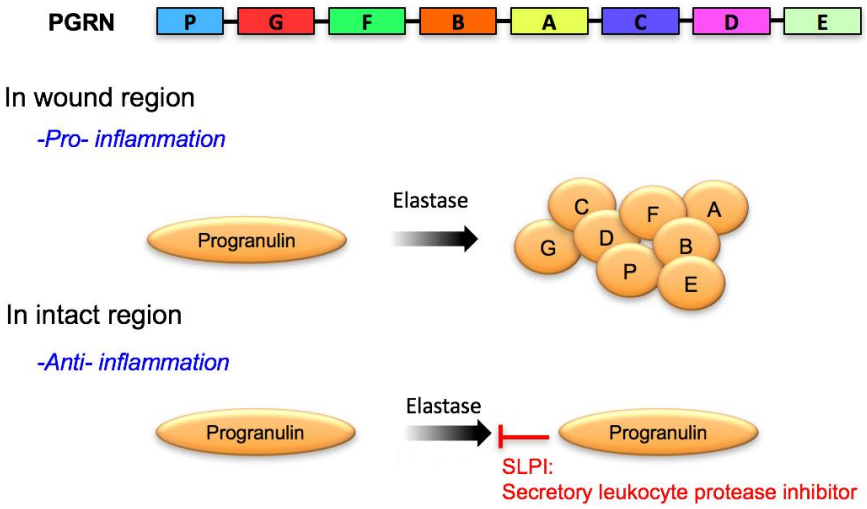

Figure 1.3. Overview of PGRN structure and granulination process. PGRN is composed of 7.5 highly homologous subunits known as granulins in top panel. At the injury site, PGRN is fragmented proteolytically into granulin peptides to promote division and migration of fibroblasts, enthothelial cells, and immune cells, while conversion of PGRN is inhibited by secreted leukocyte protease inhibitor (SLPI) at the intact site.

Similarly, Al-Maied *et al.*[36] and Brushart *et al.*[37] used a powerful stimulatory factor, electrical stimulation, which enhances neurite spouting and growth after nerve injury. Peripheral nerve regeneration is known to be promoted by brief electrical stimulation of 20 Hz for 1 hr, followed by expression of regeneration-associated genes, including α1-tubulin and GAP-43 (regeneration-associated genes; RAGs).[36] In

particular, electrical stimulation enabled synchronization of reinnnervation and acceleration of regeneration into distal stump during nerve repair.[37,38] Furthermore Demerens *et al.*[39] reported electrical stimulation induced myelin process, followed by up-regulation of myelin-related gene transcription. While encouraging as a tool for promoting regeneration, electrical stimulation in regeneration of injured nerve still remains poorly understood due to limitation of cell-type specificity for precise exploration in electrophysiological mechanisms of injured nerve.

Inspired by the effectiveness of electrical stimulation in nerve regeneration, optogenetic studies mentioned as a tool for neuroscience application, have been used, which allow precise target specificity in millisecond-timescale.[40] Optogenetics, which includes the use of light source to control cells, especially neurons, that have been genetically encoded to express light-sensitive ion channels. Optogenetic activation of neurons in both *in vivo* and *in vitro* models has been used to control many aspects in the following regions; neural circuits in amygdala,[41] mammalian behavior by regulating the activity of dopaminergic terminals,[42] and in brainstem.[43] Optogenetic activation accelerates fast light-activated channels and enzymes that allow temporally precise manipulation of biochemical and electrical proceeding by operating specific targeting mechanism. Furthermore Part *et al.*[44] showed that

optogenetic stimulation led to axon outgrowth of DRGs, which promoted expression of neurotrophic factors such as BDNF and NGF, and induced directional extension towards control DRGs, suggesting neurite chemotaxis.

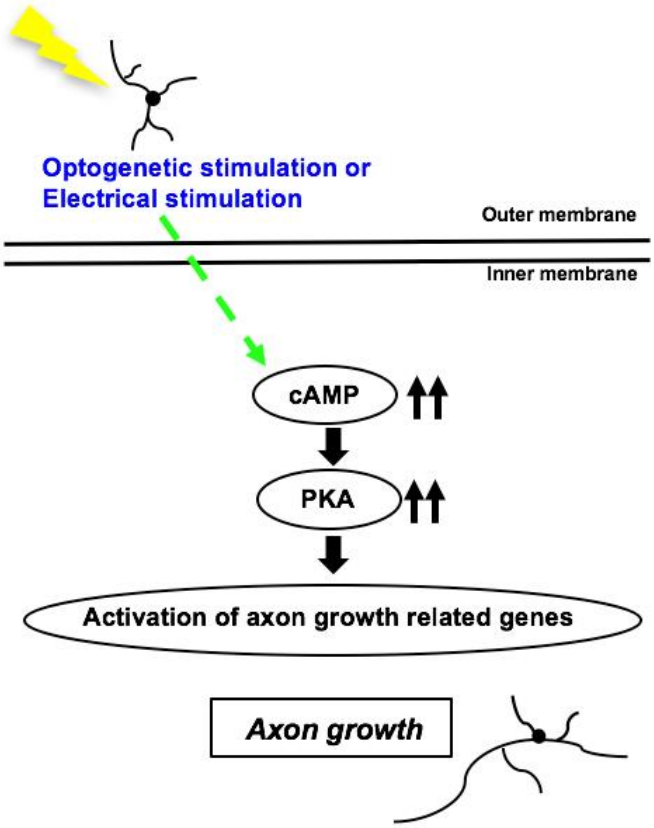

Figure 1.4. Schematic drawing summarizing the actions of axon growth by optogenetic stimulation.

Here, we first report the use of optogenetics for promoting axon growth of MNs in MN monoculture. In our study, axon growth of MNs increased by using LED stimulation and more importantly, cAMP and PKA expression levels were also activated in light excitable MNs compared with control (Fig. 1.4). Further, we investigated the utility of microfluidic biochips as a 3-D primary MN-SC coculture model; demonstrating its ability to align SCs and MN axons separated from cell bodies of MNs. We biologically analyzed the axon growth and myelin process for gene expression in MN-SC developmental coculture. Notably, this coculture model in microfluidic biochip can be used as a method to screen compounds of interest for both axon generation and myelination. In particular, we applied to optogenetics only in MN regions to induce axon growth by using LED stimulation and treated with coenzyme Q10 to stimulate myelination as previously described (Fig. 1.5).[45]

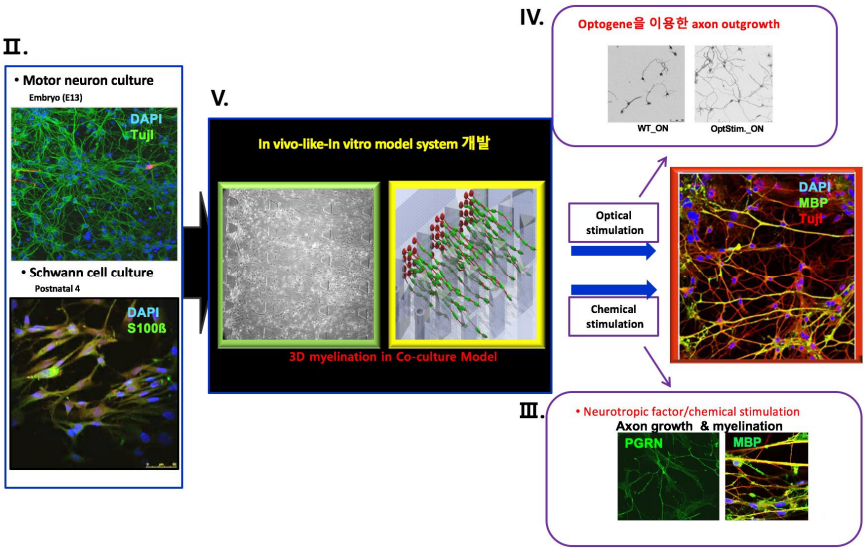

Figure 1.5. Overview of the dissertation. We established MN-SC coculture model for generation and myelination of axon from 2-D to 3-D culture using microfluidic biochip.

2. Outline of Dissertation

In this dissertation, *in vitro* coculture models of motor neurons (MNs) and Schwann cells (SCs), which can promote both axon growth and myelination for a long-term (> 1 mo) were studied. The coculture models were based on 2-D and 3-D culture using traditional culture dish and/or a custom-built microfluidic biochip. The study was focused on evaluating the long-term viability of MN as well as myelination process of MN axons as a result of the interactions between MN and SC. The study also included the effects of neurotrophic factors derived from SC and other exogenous stimulatory factors, such as chemical and electrical/optical stimuli, on MN viability and myelination.

The organization of this dissertation is as follows-Chapter I presents the theoretical background of the present study, and Chapter II the re-establishment of MN-SC coculture model in 2-D. Chapter II is focused on culture methods, including the cell sources used to generate the peripheral motor nervous system and myelination process *in vitro*. In Chapter III, the potential effects of SC on the fate of MN are presented. In particular, progranulin (PGRN), a protein secreted by SC, is presented as a new neurotrophic factor to enhance the viability and axon growth of MN. In Chapter IV, the effectiveness of optogenetics as a tool to promote axon growth of MN at lower light intensity is described. Finally, Chapter

V discusses a 3-D MN-SC coculture model based on a custom-built microfluidic biochip. This device was used to closely 3-D environment of *in vivo* mimicking *in vitro* for axon growth and myelination of MN. In Chapter VI, the conclusions and future directions for this study are summarized at the end of the dissertation.

Chapter II.

2-D Coculture of Primary Motor Neuron and Schwann Cells

1. Introduction

It is well known that primary culture of MNs alone can last only for several days in vitro because MNs are more vulnerable to oxidative stress than other types of neurons due to their high mitochondrial activity and metabolic activity.[46] Several experimental methods have recently demonstrated that primary culture of MNs can maintain its viability by the presence of SCs in the culture. Using a coculture model of MNs and SCs, Haastert *et al.*[17] reported a long-term maturation of MNs up to 3 weeks which enabled a formation of active synaptic network between MNs in vitro. Gingras *et al.*[16] presented a 3-D tissue engineering model of MN-SC coculture using a collagen-chitosan sponge.

In Chapter I, we report a coculture system comprising primary mouse MNs and SCs. In our system, MNs survived for at least 3 weeks in

culture and more importantly, SCs differentiated and formed myelin sheath around the axons of MNs. In the coculture, neurons exhibited higher viability and extended longer axons as compared to MN monoculture. By employing standard cell biological and biochemical approaches, we have confirmed that SCs myelinate MN axons within 3 weeks of coculture. The formation of myelin sheath was confirmed at the ultrastructural level. Furthermore, using the MN-SC coculture, we show that treatment with coenzyme Q10 facilitates myelination.[45]

2. Materials and Methods

A. Cell preparation

(A) Schwann cell (SC) culture

All animal experiments were conducted in accordance with protocols approved by the Institutional Animal Care and Use Committee (IACUC) at the Korea Institute of Science and Technology. SCs were isolated from sciatic nerves of CD-1 mice at postnatal day 4 (P4), as previously described.[12] Explants were incubated in Ca^{2+}- and Mg^{2+}-free phosphate-buffered saline (PBS, Lonza) containing 0.05% trypsin (Sigma) and 0.05% collagenase A (Roche) for 30 min at 37ºC, followed by centrifugation at 190 *g* for 5 min. The pellets containing tissue fragments and cells were then washed three times with high glucose-DMEM (Gibco) containing 10% horse serum (HS) (Gibco). The harvested SC pellets were suspended in SC basic culture medium composed of high glucose-DMEM, 10% HS, 4 mM L-glutamine (L-gln, Invitrogen), 100 units/mL penicillin/streptomycin (P/S, Sigma), 2 ng/mL human heregulin beta-1 (Sigma), and 1~7 μM forskolin (Sigma)(Table 1). After suspension, SCs were seeded on 12 mmϕ coverslips at a density of $3x10^4$ cells per coverslip. Prior to seeding SCs, the coverslips were coated with growth factor-reduced Matrigel (3 mm thickness on average). On DIV (days *in*

vitro) 4, complement-mediated cytolysis was performed to remove fibroblasts from SC culture. Briefly, the cells were lightly washed with 20 mM HEPES (T&I) in Ca^{2+}- and Mg^{2+}-free HBSS solution (Invitrogen), followed by washing with HMEM (high-glucose DMEM containing 20 mM HEPES buffer, 10% HS, 4 mM L-gln, 100 units/mL P/S). After washing, 4 ng/mL anti-mouse CD90 (Serotec) in HMEM was added for 15 min at 37ºC, and 200 μL of rabbit human leucocyte-associated antigens A, B, C (HLA-ABC) complement sera (Millipore) was added for 2 hrs at 37ºC. Cytolysis was terminated by washing cells with 20 mM HEPES buffer in HBSS (Table 3). After cytolysis, SCs were cultured for another three days in SC growth medium containing SC basic culture medium (described above) supplemented with 1~10 ng/mL of bFGF (Sigma) and 20 μg/mL of bovine pituitary extract (Sigma) to promote cell proliferation (Table 2). Purified SCs were characterized after complement-mediated cytolysis by confocal microscopy using GFAP, an intermediated filament protein found in non-myelinating SCs, and s100β, a marker of SCs (Fig. 2.1). Neither GFAP nor s100β was visible in fibroblasts.

Table 1. Composition of SC basic medium

Component	Concentration
DMEM	-
Horse serum	10%
L-glutamine (200 mM)	1%
Forskolin (5 mM)	1~7 μM
Human heregulin beta-1	2 ng/mL
Penicillin/Streptomycin	1%

Table 2. Composition of SC growth medium

Component	Concentration
Neurobasal medium	-
Horse serum	10%
L-glutamine (200 mM)	1%
Forskolin (5 mM)	1~7 μM
Fibroblast growth factor	1~10 ng/mL
Penicillin/Streptomycin	1%

Table 3. Complement-mediated cytolysis

Component	Concentration
Ca^{2+}-, Mg^{2+}-free Hank's balanced salt solution	-
Anti-mouse CD90 anti-Thy-1.2	4 μg/mL
HEPES buffer	5~20 mM
Rabbit Human leucocyte-associated antigens A, B, C (HLA-ABC)	-

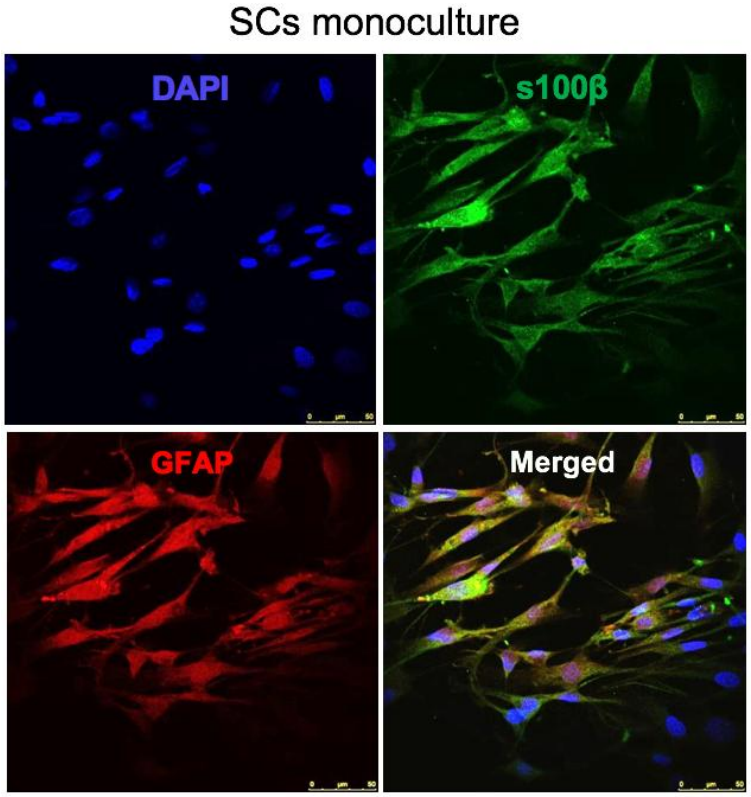

Figure 2.1. Identification of purified SCs monoculture by confocal microscopy. Double immunocytochemistry for s100β (green) and GFAP (red) in SCs isolated from the sciatic nerves of postnatal (P) 4 mice.

(B) Motor neuron (MN) culture

MNs were harvested from the spinal cord of CD-1 mice (embryonic day 14 [E14] fetus) as previously described[47] with some modifications. Ventral horns of the spinal cord (L1-L6 segment) were collected in HBSS followed by incubation with 1% TLR trypsin (Worthington) for 15

min in a 37ºC water bath, and then treated with 1% TLR trypsin inhibitor (Sigma). To extract a purified population of MNs, cells dissociated from the explant were treated for 45 min at room temperature with a selective immuno-panning dish prepared with $p75^{NTR}$ antibody solution (1:5000, Abcam) in 10 mM Tris-HCl (pH 9.5, T&I). Suspensions, including nerve fragments and $p75^{NTR}$-negative cells, were removed from panning dish by washing three times with pre-warmed neurobasal medium containing Glutamax 1 (Gibco). MNs bound to panning dish were then rinsed with depolarization solution (Table 5) containing 0.8% sodium chloride, 30 mM potassium chloride, and 2 mM calcium chloride (Merck) in distilled water for 10 s, and gently collected in MN culture medium, composed of neurobasal medium (Invitrogen), 5~10% HS, Glutamax 1, B27 supplement (Gibco), 1~10 μM β-mercaptoethanol (Sigma), and 5~20 ng/mL BDNF (Gibco) (Table 4). MNs were collected by gentle pipetting, and were then centrifuged for 5 min at 190 *g*. After centrifugation, the pellets were re-suspended in MN culture medium. Purified MNs were stained with Tau protein, present in both dendrites and axons, and TuJ1, an axon marker of neurons (Fig. 2.1).

Table 4. Composition of MN medium

Component	Concentration
Neurobasal medium	-
Horse serum	5~10%
Glutamax™-1 (100X)	1%
Beta-mercaptoethanol (1M)	1~10 μM
Penicillin/Streptomycin	1%
Brain-derived neurotrophic factor (BDNF)	5~20 ng/ml

Table 5. Depolarization solution

Component	Concentration(mM)
Potassium chloride	270~400
Sodium chloride	50~90
Calcium chloride	10~25

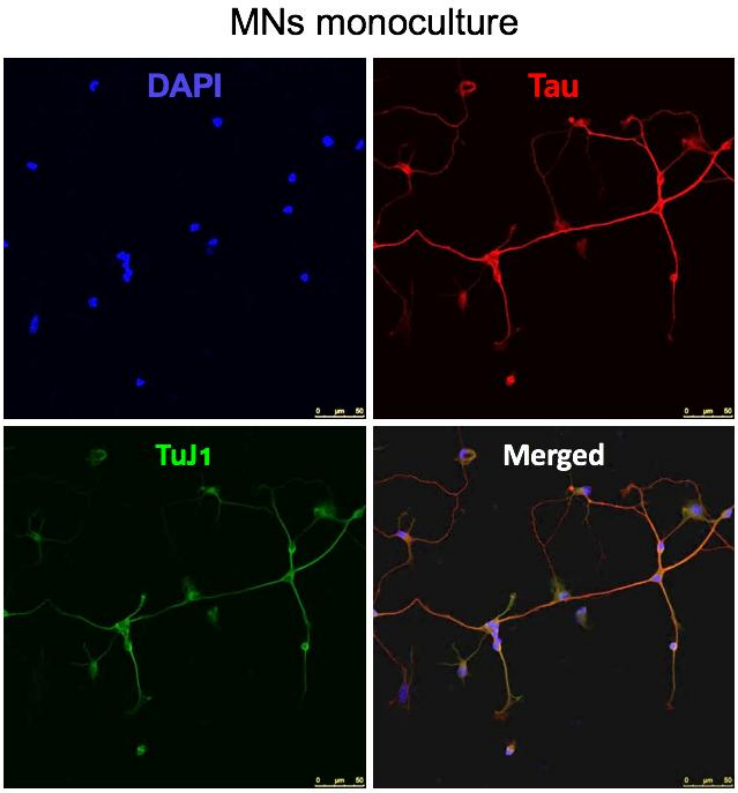

Figure 2.2. Identification of purified MNs monoculture by confocal microscopy. Double immunocytochemistry for TuJ1 (green) and Tau (red) in MNs isolated from the ventral horns of spinal cord of embryos.

(C) MN-SC Coculture on Coverslips

MNs were plated ($1x10^4$ cells/coverslip) on top of a monolayer of SC culture, which was prepared as described above (Fig 2.3). MN were seeded on SC feeder layer on which SCs cultured on growth factor

reduced-Matrigel to faciliate both migration and wrapping process of SCs around axons. To induce myelination, MN-SCs were first cultured in a coculture growth medium for 7 days, after which 25~50 μg/mL of ascorbic acid (Sigma) was supplemented for subsequent culture (Table 6). For MN monoculture, MNs were cultured directly on Matrigel-coated coverslips without SC feeder layer (Fig 2.3A). For drug treatment, cultures were treated with coenzyme Q10 (Co-Q10, 1 μM) or riluzole (0.1 μM), as indicated. After 24 hours, samples were fixed and subjected to immunostaining with the indicated antibodies. Culture medium was replenished three times a week.

Table 6. Composition of MN-SC medium

Component	Concentration
Neurobasal medium	-
Horse serum	2~6%
Glutamax™-1 (100X)	1%
B27 supplement (10X)	1X
Brain-derived neurotrophic factor (BDNF)	10~50 ng/mL
Beta-mercaptoethanol	1~5 mM
Penicillin/Streptomycin	1%
L-ascorbic acid	20~50 ng/ml

B. Measurement of cell viability

Live-Dead cell staining kit was used according to the manufacturer's instructions (Abcam). Briefly, samples were labeled with mixture of solution A (Live-Dye) and solution B (propidium iodide, PI) in the staining buffer for 15 min at 37ºC. The samples were then washed once with the staining buffer and examined under Olympus IX71 with U-RFL-T (detects FITC and TRITC). For NeuN immunostaining, cells were fixed with 4% paraformaldehyde (PFA) and treated with 0.2% Triton X-100 (Sigma), followed by blocking in 4% BSA (Millipore) at 4ºC overnight. Cells were then labeled with NeuN antibody (1:500, Abcam) for 24 hrs at 4ºC, and were stained with Alexa Fluor 488 donkey anti-mouse IgG (1:500, Invitrogen) for 1 hr at room temperature, followed by DAPI (Life Technologies) staining. The number of stained cells was counted from five random view-fields (Live-Dead cell staining and NeuN staining) of under the microscope.

C. Immunocytochemistry

All samples were fixed with 4% paraformaldehyde (PFA) for 15 min at room temperature and washed twice with PBS. The fixed samples were then soaked in PBS containing 0.2% Triton X-100 (Sigma), followed by 4% BSA (Millipore) at 4ºC overnight and labeled with the following primary antibodies: anti-Sox10 (1:500, Abcam), anti-s100β (1:500,

Abcam), anti-β-III Tubulin (TuJ1, 1:1000, Abcam), and anti-myelin basic protein (MBP, 1:500, Abcam). All samples with primary antibodies were incubated in 1% BSA with PBS at 4ºC overnight. The samples were then washed with PBS containing 1% BSA twice, and incubated with goat anti-chicken IgY H&L (1:1000, Abcam), goat anti-rabbit IgG H&L (1:500, Abcam), or Alexa Fluor 488 donkey anti-mouse IgG (1:500, Invitrogen). The nuclei of cells were stained with DAPI (Life Technologies) for 15 min at room temperature. Fluorescence of the culture was visualized under a confocal microscope (Zeiss LSM 700).

D. Measurement of axon length

In Chapter II, cultures were fixed and labeled for TuJ1 to visualize axons of MNs, and the lengths of axons were measured by using ImageJ software (100 axons/coverslip, N=3).

E. Quantitative analysis of pre-myelinating and myelinating Schwann cells

During 2-D coculture, cultures immunostained with anti-MBP antibodies showed two distinct patterns of MBP expression: pre-myelinating SCs showed relatively wide-spread expression of MBP adjacent to the axons while myelinating SCs showed highly localized expression of MBP along the axons. Cocultures were stained with MBP and TuJ1 at DIV 10,

14, and 21 and the proportion of these two types was calculated from six different fields of view under confocal microscope.

F. Western blot assays

Expressions of MBP and Krox20 were quantitatively analyzed by using western blot analysis. The cells at DIV 1, 7, 14, and 21 were lysed in RIPA buffer containing 1% SDS and protease inhibitor (aprotinin, leupeptin, pepstatin A, PMSF). The protein concentration of cell lysates was measured by using Bradford assay. The samples were prepared in an SDS sample buffer, heated for 3 min at 98ºC, and 6 μg of the protein from each sample were loaded in SDS loading buffer and then transferred to a PVDF membrane. The membranes were blocked in 2.5% skim milk for 1 hr, followed by incubation with anti- rabbit Krox20 (1:1000, Abcam) or anti-rat MBP (1:500, Abcam) antibodies at 4ºC overnight. The membranes were washed three times in TBST and incubated with goat anti-rabbit and anti-rat IgG conjugated with horseradish peroxidase (1:1000, Sigma) for 2 hrs. Bands were visualized by using the ECL system. The intensity of the blots was quantified with ImageJ software.

G. Transmission electron microscopy

At DIV 14 and 21, cultures were fixed with 4% glutaraldehyde in PBS and stored at 4°C overnight, and post-fixed with 1% osmium tetroxide

for 30 min. Samples were embedded in pre-epoxy resin before dehydration with a series of ethanol solutions (70%, 80%, 85%, 90%, 95%, 100%). Sections were taken between 70~80 nm using Ultramicotome (Leica, Ultra Cut C) and picked up on copper grids, and stained in uranyl acetate and lead citrate. Images were acquired with Cryo-TEM (FEI, CryoTecnai F20).

H. Statistical analysis

Average data were shown as mean ± standard error, and the comparison between different groups was performed by using repeated measures analysis of variance (ANOVA). Statistical significance was set at a value of $*p < 0.05$, $**p < 0.01$, $***p < 0.001$.

3. Results

A. Establishment of a 2-D MN-SC coculture model

To develop a long-term culture model of MNs, SCs were harvested from the sciatic nerves of postnatal day 4 (P4) mice and cultured on approximately 3 mm-thick Matrigel. SCs were cultured for a week until cells formed a confluent feeder layer. On top of SC feeder layer, purified MNs obtained from the ventral horns of gestation day 14 embryos (E14) were seeded and cocultured (Fig. 2.3B, MN-SC coculture). As a control, MNs were cultured directly on Matrigel without prior culture of SCs (Fig. 2.3A, MN monoculture). In the MN monoculture, MNs extended axons up to DIV 7, but neurons gradually degenerated thereafter and by DIV 14, few MNs survived (Fig. 2.4). By contrast, in the MN-SC coculture, neurons differentiated and developed neurites and remained intact up to at least DIV 21. On DIV 3, we detected the migration of SCs toward the axons of MNs and on DIV 7, and observed nuclei of SCs around the axons.

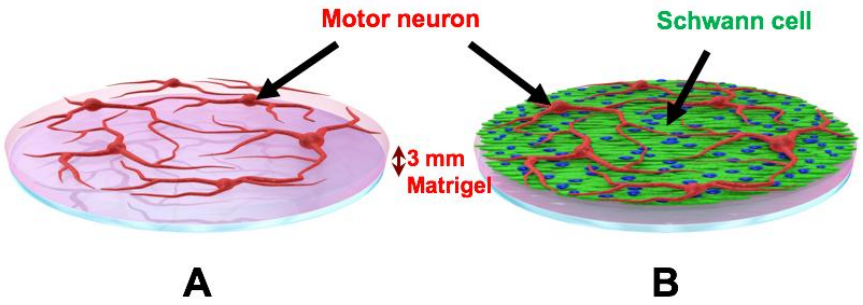

Figure 2.3. Schematic illustration of MN monoculture and MN-SC coculture on a Matrigel. (A) MNs cultured on a coverslip coated with growth factor-reduced Matrigel. (B) MNs cultured on a SC feeder layer that grew up to 90% confluency.

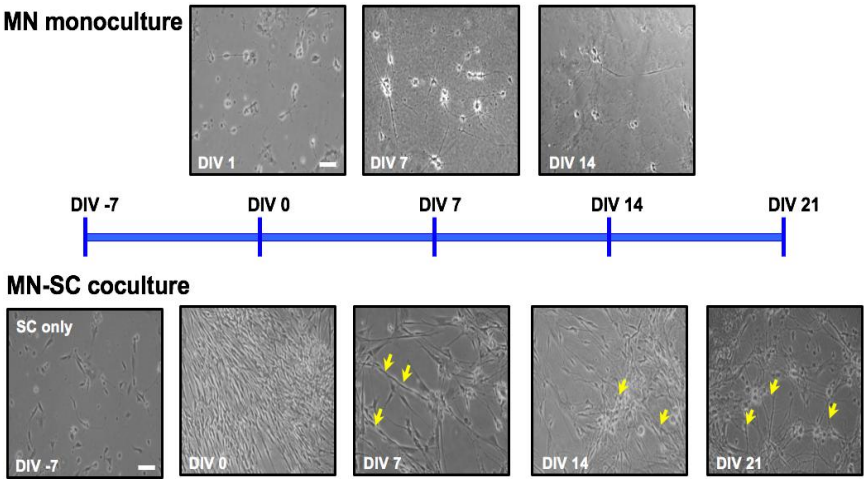

Figure 2.4. Flowchart of differentiation of MNs in culture. Representative light microscopic images of MN monoculture and MN-SC coculture at different stages are shown. In MN monoculture, purified neurons form synapses at DIV 7, but viability greatly reduces by DIV 14. In MN-SCs coculture, SCs are cultured for 7 days, and then MNs were grown on top of the SC feeder layer. MNs in the coculture survive for at least 3 weeks and motor axon diameter increases (arrows, yellow). All images are at the same scale. Scale bar, 50 μm.

B. MN cell viability in both monoculture and coculture

We also compared cell viability in MN monoculture and MN-SC coculture systems by using Live-Dead cell staining kit and NeuN-DAPI double staining methods (details in Methods section). In the MN monoculture, vast majority of neurons (96%) failed to survive (Figs. 2.5A and B). However, the MN-SC coculture showed almost no cell death up to DIV 21 (Fig. 2.5C). Furthermore, the viable MN cell number was maintained throughout the culture, whereas the viable SC cell number steadily increased up to DIV 21 (Fig. 2.5D), suggesting that SCs play a critical role in supporting the survival of MNs.

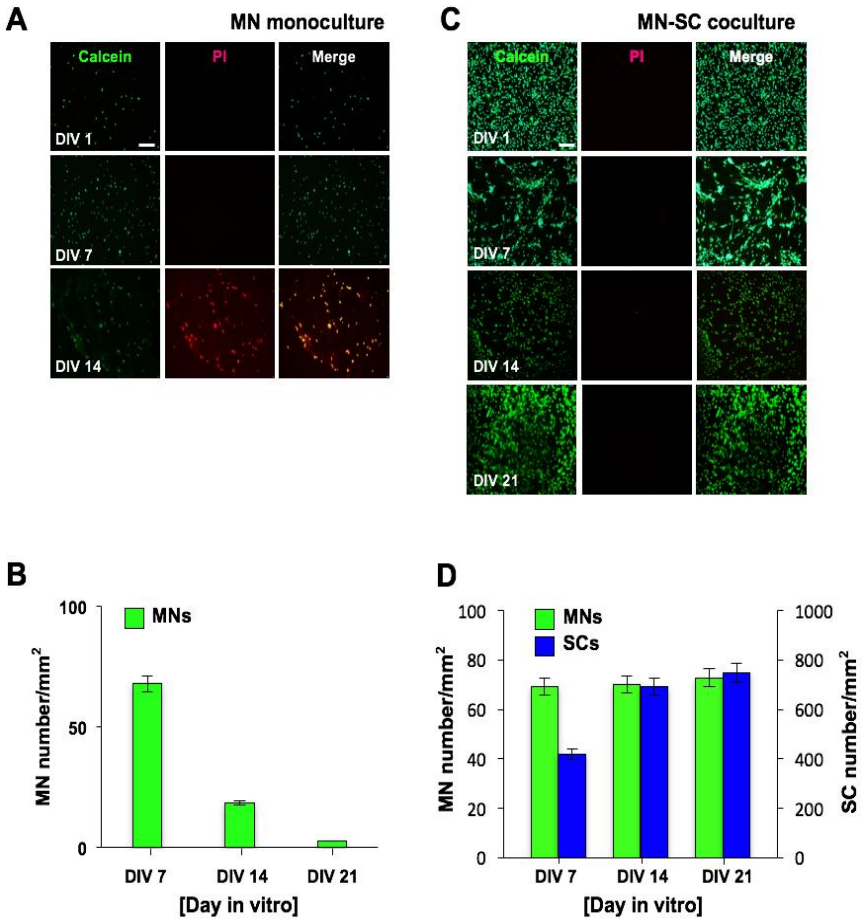

Figure 2.5. Cell viability in MN monoculture (A and B) and MN-SC coculture (C and D). Viability was assessed by double-staining with calcein-AM and propidium iodide (PI) at DIV 0, 7, 14, or 21, as indicated (A and C). Samples were then fixed and immunostained with DAPI and NeuN antibody (B and D). Representative images (A and C) and quantification of NeuN-positive MNs are shown (B and D). n=5; scale bar, 100 μm.

C. Axon length of MNs in monoculture and coculture

We next quantitatively examined the effects of SCs on axon outgrowth of MNs using TuJ1 staining for nerve fibers, and ImageJ to quantify the fiber length (Fig. 2.6). When axon length was measured at 2 days after plating MNs (Fig. 2.6A), average axon length of MNs grown in the MN-SC coculture system was about 4 times longer than that in the MN monoculture. In the MN-SC coculture, axons grew at a rate of about 50 μm per day, which is consistent with a previous report.[13] Taken together, these results suggest that SCs are essential for the survival and neurite outgrowth of MNs.

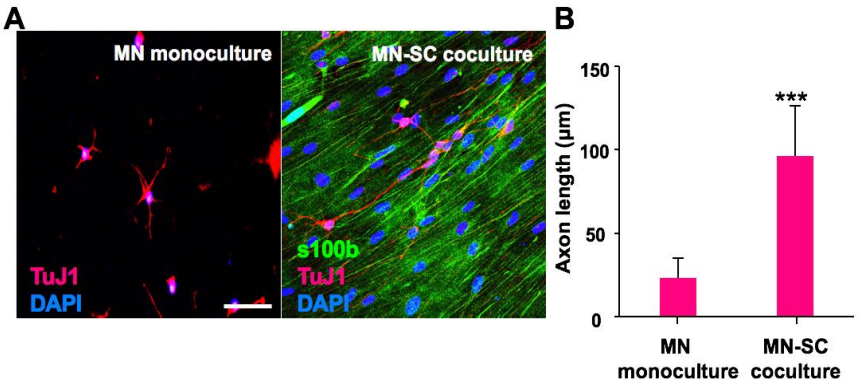

Figure 2.6. Axonal outgrowth in MN monoculture and MN-SC coculture. (A) Confocal images of MN monoculture and MN-SC coculture are shown. Cells were fixed and stained for s100β, TuJ1 and nucleus (DAPI), as indicated, at DIV 2, and lengths of axons were measured. Scale bar, 50 μm. (B) Each bar represents mean ± S.E. value. n=100; *** $p < 0.001$.

D. Myelination of MNs

To investigate if SCs differentiate and, more importantly, myelinate MN axons in our MN-SC coculture system, cultures were examined for expression of markers of SC differentiation and myelination, such as myelin basic protein (MBP), SRY-related HMGbox-10 (Sox10) and Krox20. We found that the expression of Sox10, a transcription factor which controls myelination in the PNS,[48] was detected in the soma of SCs on DIV 7 and increased thereafter (Fig. 2.7). Expression of MBP

was detected on DIV 10, and eventually became highly localized along the axon fiber by DIV 14 (Fig. 2.7, green). Western blot analysis confirmed the expression of MBP and Krox20, a transcription factor induced by the activation of Sox10. Krox20 is known to suppress the immature state and promote myelination.[49,50] We observed an increase of both MBP and Krox20 protein levels over time (Fig. 2.8), consistent with our immunocytochemistry results (Fig. 2.7).

Next, we examined myelin sheath formation on DIV 21 in detail by confocal microscopy and transmission electron microscopy (TEM). Z-stack images of confocal microscopy confirmed tight interaction between MBP and axons of MNs (Fig. 2.9). By taking TEM images, we confirmed that SCs formed loose sheaths by DIV 14, which could be the premyelination stage (Figs. 2.10A and B), and that SCs tightly wrapped the nerve fiber by DIV 21, which could be the completed myelination stage (Figs. 2.10C and D). The thickness of compact myelin sheaths was approximately 0.2 μm at DIV 21.

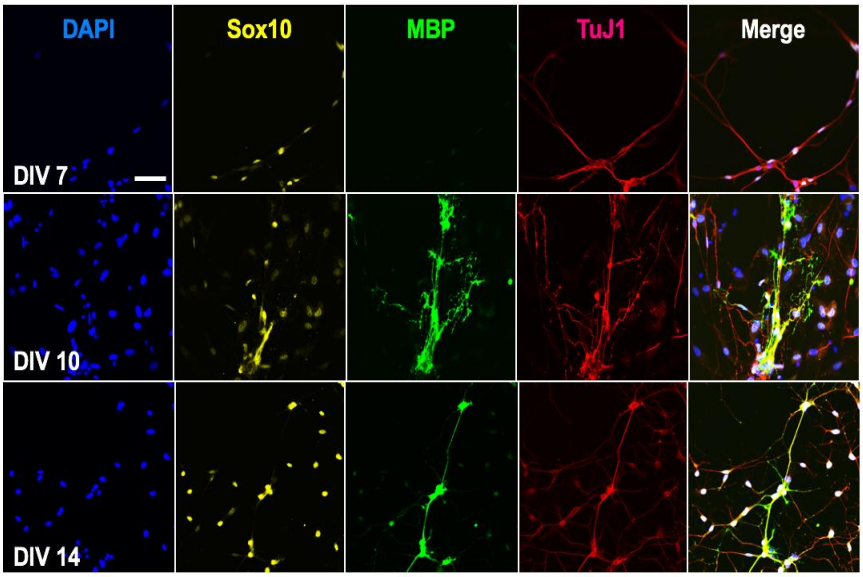

Figure 2.7. Differentiation of neurons and SCs in MN-SC coculture. Representative confocal images of MN-SC coculture are shown. Cells were fixed and stained for Sox10, MBP, TuJ1 and nucleus (DAPI) at DIV 7, 10, and 14, as indicated. Note the expression of MBP protein around axons at DIV 10 and 14. Scale bar, 50 μm.

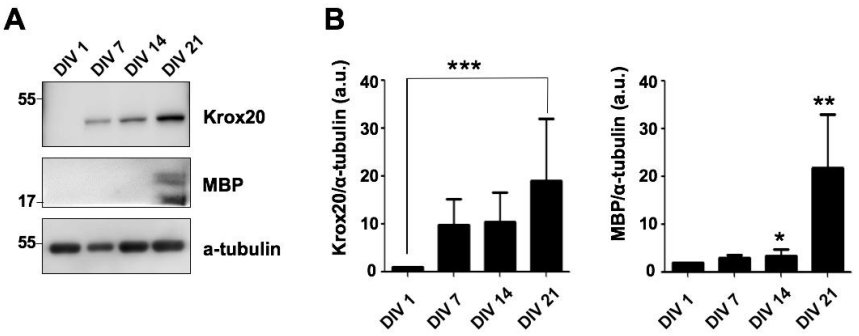

Figure 2.8. Increased expression of Krox20 and MBP protein in MN-SCs coculture. The levels of Krox20 and MBP were determined by western blot analysis at DIV 1, 7, 14, and 21, as indicated. Representative blots (A) and quantification (B) of Krox20 and MBP levels are shown.

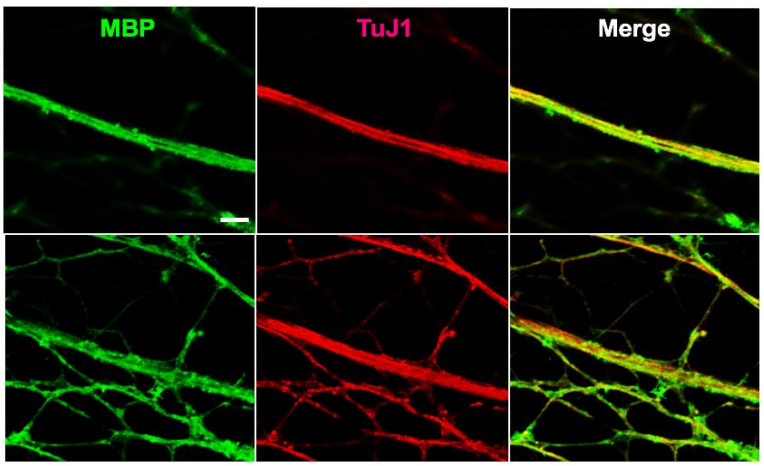

Figure 2.9. Formation of compact myelin sheaths in the MN-SCs coculture model. At DIV 21, cultured cells were observed by confocal microscopy after immunolabeling with anti-MBP (1:500, green) and anti-TuJ1 antibodies (1:1000, red). Images shown at the top and bottom panels are serial images collected throughout z-sections. Scale bar, 5 μm.

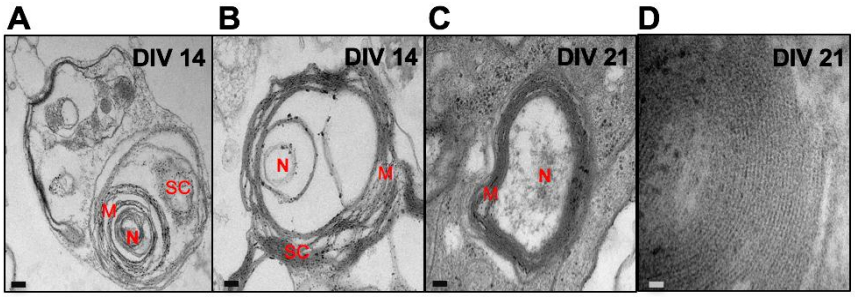

Figure 2.10. Myelination of axons in the MN-SC coculture model. The extent of myelin sheaths was analyzed by transmission electron microscopy at DIV 14 and 21. Micrographs from DIV 14 show SCs loosely wrapping around the nerve fiber (A, B), whereas those from DIV 21 clearly show the formation of compact myelin sheaths (C). (D) Representative image shows a heavily myelinated nerve fiber. Scale bar, 200 nm (A-C), 20 nm (D). N, nerve fiber; m, myelin sheaths.

E. Distinct stages of myelination observed in the 2-D MN-SC coculture model

It is well-known that oligodendrocytes in the CNS differentiate from premyelinating to myelinating stage, and the transition is controlled by several intrinsic and extrinsic signals.[51] Likewise, in our MN-SC coculture system, SC myelination proceeded through two distinct stages, which could be distinguished on the basis of MBP expression pattern and interaction with axons as mentioned above in the TEM images. In the premyelinating stage, expression of MBP in SCs was relatively widespread, whereas in the myelinating stage, MBP expression in SCs was tightly localized along the axons. By counting the number of these two different types of SCs under confocal microscope, we found that while most SCs were at pre-myelinating stage on DIV 10. The number of myelinating SCs gradually increased in culture and reached 80% by DIV 21 (Fig. 2.11B).

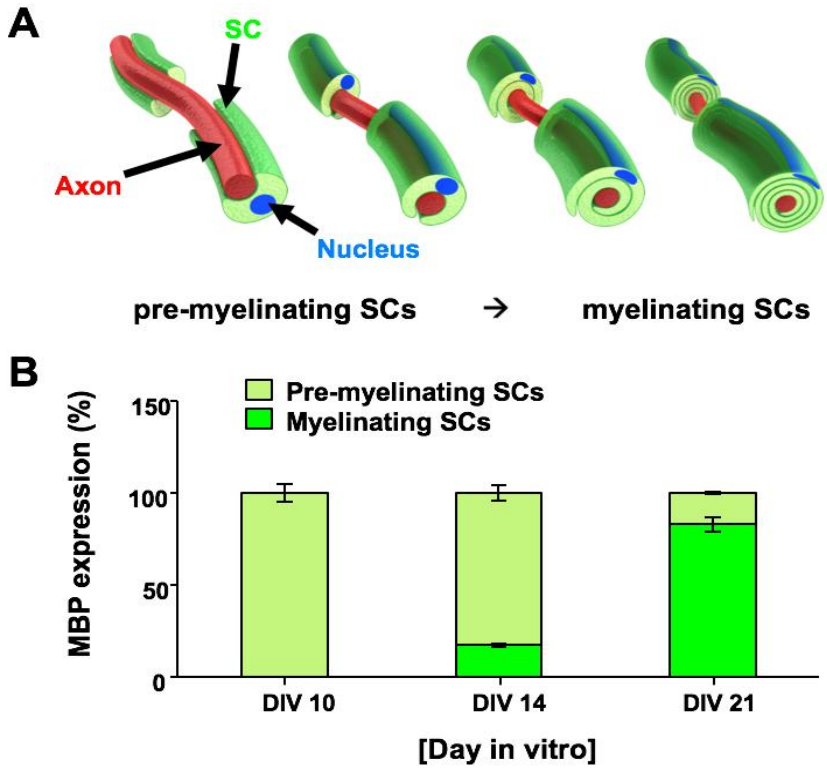

Figure 2.11. Pre-myelinating and myelinating SCs. (A) The process of myelination. SCs envelop an axon and continue to produce myelin. SCs then wrap their plasma membrane loosely around an axon, yielding in multiple successive layers. Membrane wrappings are compacted into a tightly packed insulation coat. (B) SCs in culture were fixed and stained for MBP at DIV 10, 14, and 21, as indicated. MBP-expressing SCs were categorized into two groups, pre-myelinating and myelinating (n=5).

F. Promotion of MN myelination by coenzyme Q10

We next treated our coculture samples with drugs implicated in the treatment of neurological diseases. Samples were treated with riluzole (2-amino-6-trifluoromethoxy benzothiazole), an FDA-approved drug for the treatment of amyotrophic lateral sclerosis (ALS),[52] a debilitating neuromuscular disease which involves the death of motor neurons; or with coenzyme Q10 (Co-Q10) (1,4-benzoquinone, also known as ubiquinone), an antioxidant and mitochondrial cofactor, which has been considered as a potential therapeutic agent for demyelinating and neurodegenerative diseases.[53,54] As shown in Figs. 2.12A and B, Co-Q10 treatment facilitated MBP expression and increased the number of myelin-forming SCs as compared to control. At DIV 7, MBP expression was detected only in Co-Q10-treated cultures but not in control or riluzole-treated cultures. By DIV 14, MBP expression was also detected in control and riluzole-treated cultures, but the percentage of myelinating SCs was lower as compared to Co-Q10-treated cultures. By DIV 21, all cultures expressed MBP. We detected an increase of Krox20 expression in all cultures, demonstrating that SCs differentiate properly in our MN-SC coculture system, and that treatment of riluzole or Co-Q10 did not affect the transition from premyelinating to myelinating stage *per se* but perhaps controls later stages of SC myelination (Fig. 2.12C).

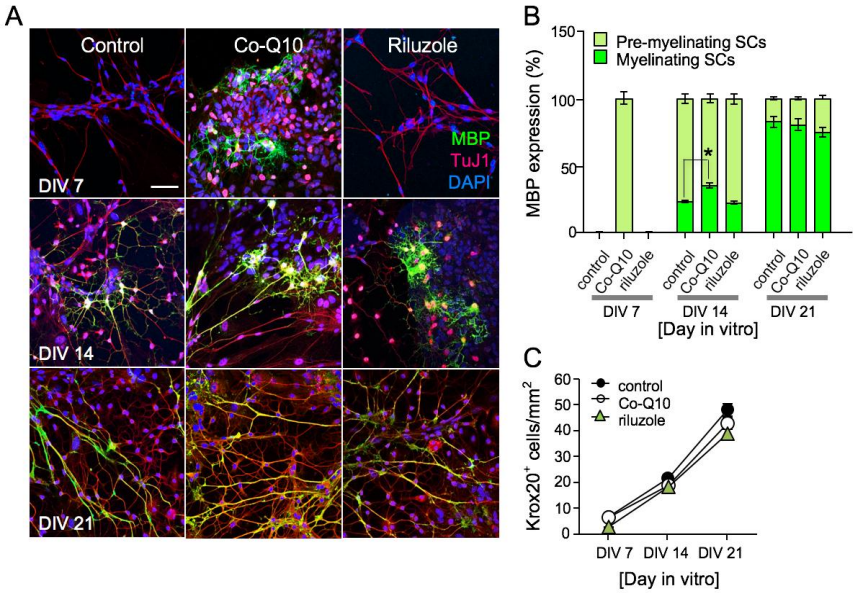

Figure 2.12. Effects of drug treatment on myelination. Comparison of MBP expression in MN-SC coculture treated with coenzyme Q10 (Co-Q10) or riluzole using immunocytochemistry. Note the marked elevation of pre-myelination in cultures treated with Co-Q10 at DIV 7. n=5; **p* < 0.05; scale bar, 20 μm.

Chapter III.

Progranulin (PGRN), A Novel SC-Secreting Protein: Effects on Viability and Axon Growth of Motor Neuron.

1. Introduction

Many studies[25,55] have reported that SCs produce a wide variety of neurotrophic factors, which are critical for the viability and myelination of peripheral neurons as well as for their repair after injury. For example, Henderson *et al.*[56] reported that glial cell line-derived neurotrophic factor (GDNF) produced by SCs is an important survival factor for MNs in culture. Later, it was reported that when sciatic nerve was subjected to a chronic injury, GDNF mRNA was rapidly upregulated in SCs around the injury site.[57] SC is also known as a rich source of brain-derived neurotrophic factor (BDNF), nerve growth factor (NGF), and ciliary

neurotrophic factor (CNTF).[26] BDNF promotes nerve regeneration by enhancing axon branching and arborization of neuron[27] and also by upregulating IL-6 expression by SCs.[58] CNTF was proven not only to support viability of MN but to prevent degeneration of MN after injury.[59] Recent studies reported progranulin (PGRN) as a potential neuroprotective growth factor to support the survival of MN[35] and also as a potent regulator of neuronal differentiation and outgrowth.[34]

In Chapter III, using a transwell culture model of MN and SC, we examined the role of progranulin (PGRN) as a potential neurotrophic factor to promote the cellular viability and axon growth for MNs.

2. Materials and Methods

A. MN-SC coculture on transwells

Viability of MNs controlled by SC-secreted proteins was analyzed by using transwells. Transwells were pre-coated poly-l-lysine (PLL) solution for 3 hrs at 37˚C, and then initially equilibrated by adding culture medium for at least 1 hr before SC seeding in the upper transwell inserts (1.5 x 10^4 cells/transwell insert). One day after SCs seeding, coverslips seeded with MNs (1 x 10^4 cells) were placed onto the lower 6 wells. Coculture medium composed of neurobasal medium with 2~10% HS, 2 mM L-Gln, 1X B27 supplement, 10 μg/mL BDNF, 5 μM forskolin and 1 mg/mL pituitary extract bovine. To test the viability of MNs on transwell coculture, we were treated it with SLPI (100 nM, PROSPEC, USA) on coculture medium. The co culture medium was changed three times a week.

B. Mass spectrometric assays

Identification of protein was performed by in-gel digestion using PGRN-containing gel pieces cut from SDS-PAGE gels. The procedure followed as previously described.[60] The tryptic peptide was analyzed using a LTQ XL-Orbitrap mass spectrometer (Thermo Scientific, San Jose, CA, USA) coupled with an Eksigent nanoLC-ultra 1D plus system at a flow rate of

300 nL/min, with a linear gradient of acetonitrile from 5% to 40% in water in the presence of 0.1% formic acid over a period of 40 min. The spray voltage was set to 1.9 kV, and the temperature of the heated capillary was set to 250°C. The instrument cycled through acquisition of a full scan (m/z 300–2,000) followed by 10 data-dependent MS/MS scans coupled with a predefined inclusion list including the m/z values of proteotypic peptides for PGRN (isolation width, 2 m/z; normalized collision energy, 27%; dynamic exclusion duration, 30 s). The acquired MS/MS spectra were searched against composite Uniprot mouse (Jan 2015 release) with horse albumin and NCBI mouse PGRN sequence database using SEQUEST in Proteome Discoverer 1.4 (Thermo Fisher Scientificion, version 1.4.0.288).[61] Two trypsin-missed cleavages were allowed and the peptide mass tolerances for MS/MS and MS were set to ±0.5 and ±15 ppm, respectively. Other options used for SEQUEST searches were fixed modification of carbamidomethylation at cysteine (+ 57.0215 Da), variable modifications of oxidation at methionine (+ 15.9949 Da).

C. Gene transfection

To measure axon growth dependent on PGRN concentration and SLPI concentration, at DIV 4 after seeding, MNs were transfected with tdTomato (1 μg/coverslip) for 1 hr in 37˚C incubator using CalPhos

mammalian kit (Clontech Laboratories, Inc.) as previously described[62] with some modifications. Briefly, the mixture of 1 μg/mL DNA in culture medium containing 0.04 M $CaCl_2$ and 2X HBSS solution were incubated for 30 min at room temperature. The DNA/Ca^{2+}-phosphate suspension was added on MNs that were cultured on coverslips and incubated for 90 min at 37°C incubator. After incubation, DNA/Ca^{2+}-phosphate precipitates were removed by adding new MN culture medium that was pre-equilibriated in 10% CO_2 incubator for at least 30 min.

D. Measurement of axon length

In chapter III, tdTomato-transfected MNs were labeled for TuJ1 to measure co-labeled axons and measured by using ImageJ software (10 axons/coverslip, N=5).

3. Results

A. MN viability on transwell coculture model

We initially examined whether the viability of MNs were controlled by SC-secreting protein or not. We cocultured primary SCs grown in the upper chamber of transwell inserts with MNs cultured on coverslips in the lower chamber of transwell insert (Fig. 3.1A). As previously reported,[45] we found that neurotrophic factors released by SCs also promote the viability of MNs compared with MN monoculture, using live and dead staining kit (Figs. 3.1B and C). However, the viability of MN cultured on transwell was lower than that of MNs cultured on SC feeder layer (Figs. 3.1C and D). Furthermore, we observed that these effects attenuated to about 46% by addition of SLPI (100 nM) on DIV 14 (Figs. 3.1B and C). These results suggest that neurotrophic protein released by SCs is critical to maintain the viability of MNs, and this viability effect can be abolished by SLPI.

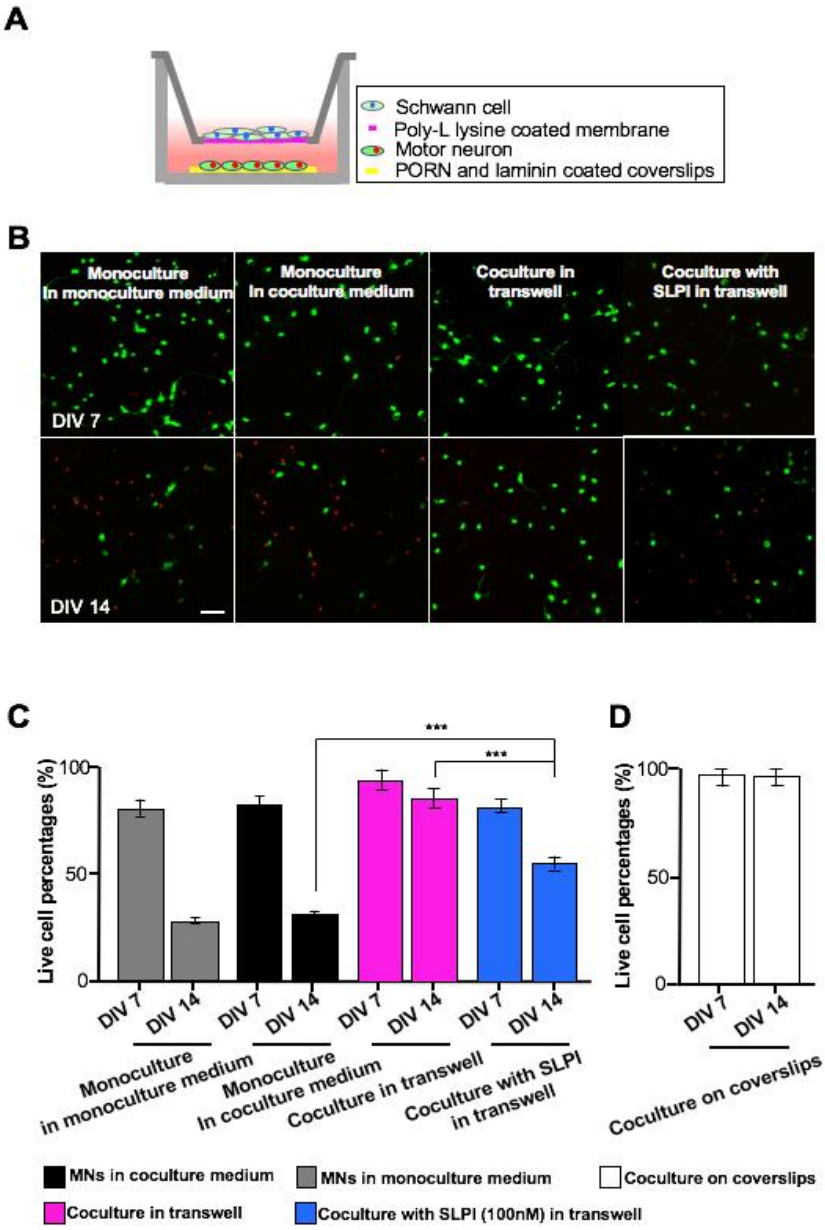

Figure 3.1. Cell viability was compared between MN monoculture and MN-SC coculture using transwell. (A) Diagram of transwell coculture. MNs in lower compartment that cultured on coverslips pre-coated with PORN and laminin, whereas SCs in upper compartment were plated on PLL pre-coated membrane. (B) The cultures were double-stained with calcein-AM and propidium iodide (PI) at DIV 7 and 14 to evaluate cell viability. (C and D) Viability of MNs was quantified by counting the number of live (stained in green) and dead (stained in red) cells under fluorescence microscope. Each bar represents mean ± S.E. value. (n=3, 5 random regions), ***$p < 0.001$, Scale bar, 50 μm.

B. Identification of PGRN secreted by SCs

We next examined whether PGRN is secreted from SC or not. To identify PGRN in media, primary SC were cultured in medium supplemented with 10% HS for 72 hrs to stabilize cells after seeding, and then culture medium was serially diluted into serum-free condition (Fig. 3.2A). Through LC-MS/MS, PGRN were identified from 4 peptide sequences (HCCPGGFHCSAR, VHCCPHGASCDLVHTR, AVSLPFSVVCPDAK, and LPDPQILK) in conditioned medium without serum (Fig. 3.2B).

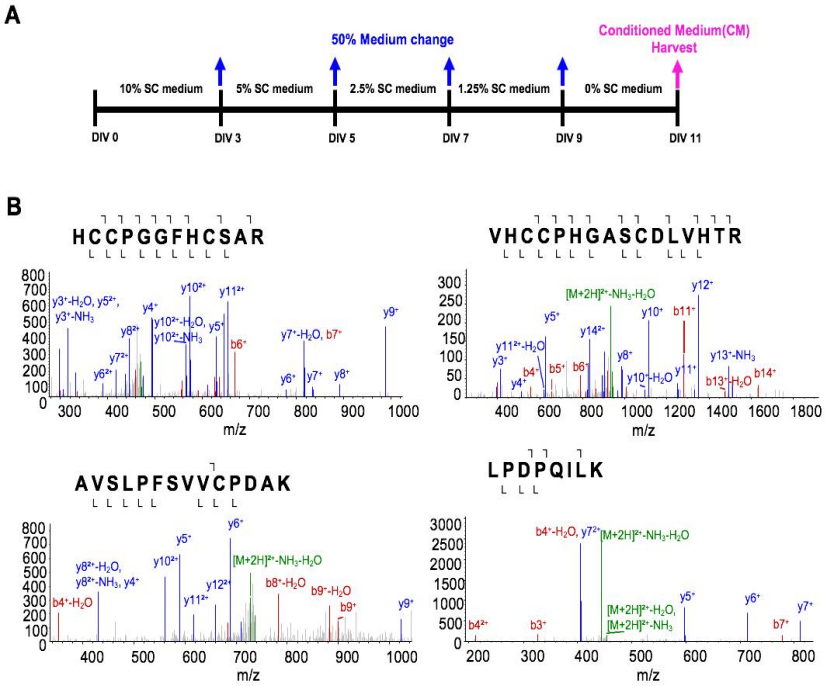

Figure 3.2. Identification of PGRN secretion in SCs conditioned medium using Liquid Chromatography-Tandem Mass Spectrometry. (A) Flowchart of cell culture to harvest of the supernatant derived from SCs. The medium was changed and diluted in half with serum-free medium serially (every two days after DIV 3). (B) PGRN was identified with 4 peptides in serum-free media (FDR < 1%).

C. Regulation of PGRN secretion by SC culture conditions

To investigate if PGRN expression level were controlled by SC culture conditions such as dependency on time and serum concentration, we examined expression levels of PGRN as well as markers of SC differentiation, such as Krox 20.

- *Day-dependent conditions*

We first examined PGRN expression levels during SC proliferation. To quantify PGRN levels, we seeded SCs at different densities on culture dishes to acquire the same number of cells when SCs were harvested on DIV 1, 3, 7, and 14. Half of the culture medium was exchanged every two days, and SCs were incubated with fresh medium for 1 day before obtaining samples (Fig. 3.3A). We observed an increase in the PGRN and Krox20 protein levels over time using western blot analysis, and the average PGRN and Krox20 expression levels were 1.5 and 3.13-fold higher than that of DIV 1, respectively (Fig. 3.3B).

- *Serum levels*

We next examined the PGRN protein level under different serum concentration in SC culture medium. To acquire each culture samples, SC culture media were diluted by exchanging 50% serum-free medium every day at DIV 3 after stabilization of SCs. At DIV 6, SCs were washed with PBS once and the medium in each condition was exchanged before cell lysates were harvested (Fig. 3.4A). We found that PGRN protein level was higher in 10% horse serum condition than in 0% horse serum condition. Furthermore, we confirmed that Krox20 expression levels were also increased with horse serum condition (Fig. 3.4B). These results demonstrated that PGRN expression was increased under SC serum culture condition, with a concurrent increase in Krox20 expression.

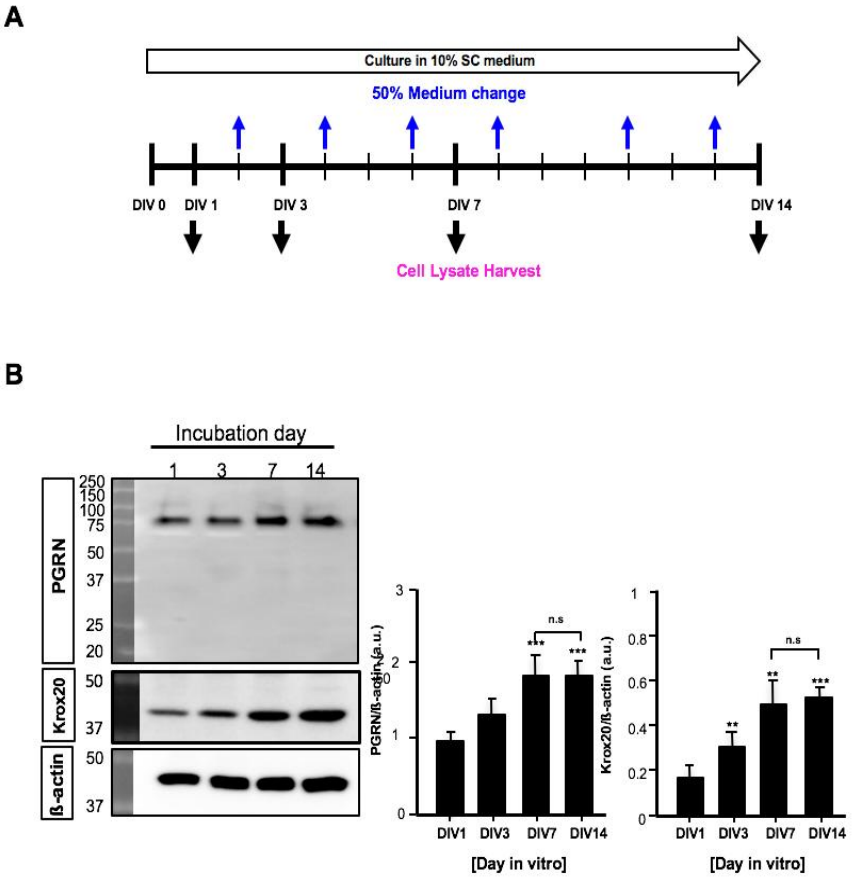

Figure 3.3. Increase in PGRN secretion by day-dependent SCs. (A) Schematic procedure of preparation of cell lysates at day 1, 3, 7 and 14 to analyze protein levels of PGRN and Krox20. (B) Representative blots (left) and quantification results (right) are shown. Each bar represents mean ± S.E. value. n=5, 10 axons/ each group; *$p < 0.05$, **$p < 0.01$, *** $p < 0.001$.

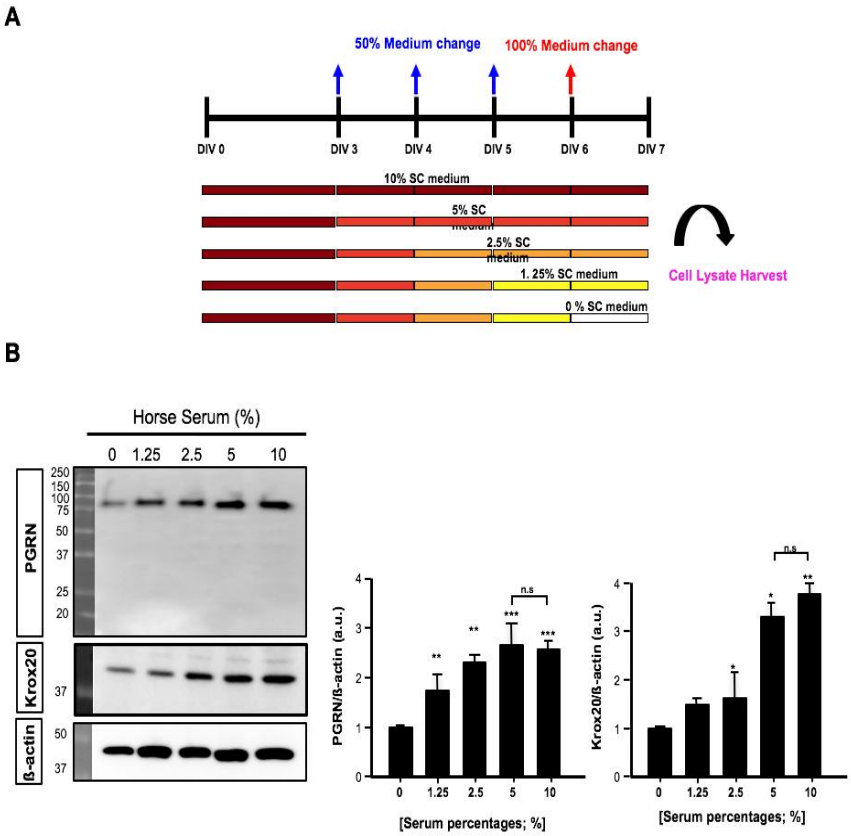

Figure 3.4. Increased expression of PGRN by serum levels-dependent SCs. (A) Schematic procedure of preparation of SCs lysates from SCs cultured in different serum levels (10%, 5%, 2.5%, 1.25% and 0% serum) at DIV 7 to analyze protein levels of PGRN and Krox20 (C). Each bar represents mean ± S.E. value. n=5; *$p < 0.05$, **$p < 0.01$, *** $p < 0.001$.

D. Exogenous PGRN enhances viability and axon growth of MNs

To explore the neurotrophic properties of PGRN, we evaluated whether axon growth of MNs was regulated by PGRN in a dose-dependent manner. We used tdTomato transfection using calcium phosphate methods at DIV 5, which enabled us analyze precisely a single axon of MN. At DIV 6, fixed MNs were immunostained with TuJ1 and tdTomato-TuJ1 stained axons were counted using ImageJ (Fig. 3.5A) We identified that axon growth improved significantly with treatment of recombinant PGRN ranging from 0.01 nM to 10 nM in MN monoculture at DIV 6, wherein rPGRN was added on day 0 in cultures (Fig. 3.5B, top panel). The elongation of axons was about 1.5- fold more in 1 nM rPGRN (236.973 ± 24 μm) condition, compared to control (144.483 ± 10 μm). We did not observe a significant increase when rPGRN concentration was above 1 nM (Fig. 3.5C, left panel). Furthermore, these neurotrophic effects of rPGRN were attenuated by adding rSLPI at different concentrations. Treatment of rSLPI on growth-promoting effects of rPGRN have decreased axon length of MN with increasing SLPI concentration, especially, MNs treated with 10 nM SLPI (129.096 μm) that have short axon length similar to that of control MNs (144.486 μm) (Fig. 3.5B, bottom panel, and 5C, right panel).

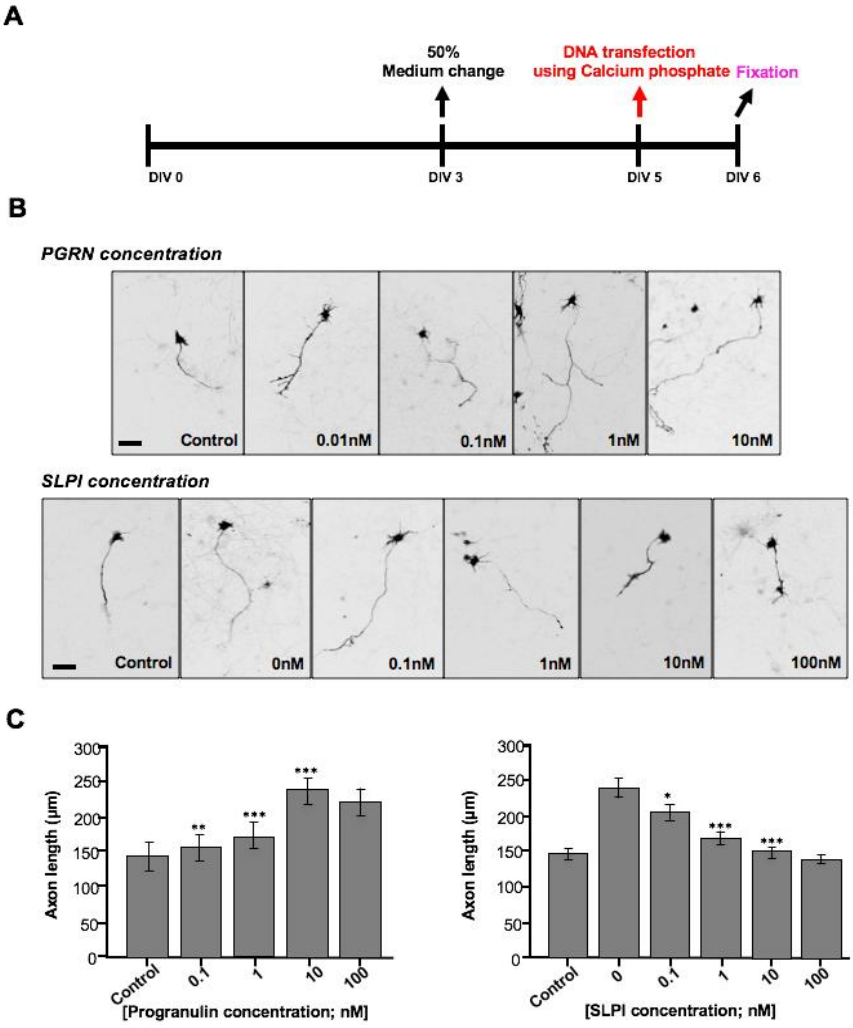

Figure 3.5. Axon growth of MN was dependent on the concentrations of PGRN and SLPI, a molecule that deactivates PGRN by blocking the hydrolysis of the protein. (A) tdTomato gene was transfected in MNs using DNA-calcium phosphate method to visually identify the axon outgrowth. (B) Representative images of tdTomato-MNs demonstrating axon growth as a function of PGRN and SLPI concentrations. (C) Axon length of MNs shown in (B) was measured using ImageJ software. Note that axon length of MN increased with an increase in PGRN concentration, but decreased with an increase in SLPI concentration. Each bar represents mean ± S.E. value. n=5, 10 axons/ each group; *p < 0.05, **p < 0.01, *** p < 0.001. Scale bar, 50 μm.

E. Effects of PGRN fragments on MNs

We next sought to determine which PGRN fragment promoted viability and axon growth of MN. Previous studies in MN monoculture have suggested that MNs did not survived after DIV 14 without SC.[16,45] However, we found that exogenous PGRN treatment promoted MNs viability (62%) at DIV14 in MN monoculture compared with that of control. In particular, both GRN C (72%) and GRN E (74%) significantly improved MNs viability at DIV14, confirming that GRN C and GRN E of PGRN fragment have neurotrophic properties (Fig. 3.6A and B).

Zhu *et al.*[63] reported that SLPI blocked PGRN processing by direct binding to PGRN and by inhibition of elastase-mediated digestion that converts PGRN to PGRN fragments during wound healing. We therefore

examined the effect of SLPI on both PGRN and PGRN fragments and observed that co-administration of SLPI prevented the neurotrophic properties of PGRN in MN monoculture at DIV 14. However, we found that SLPI interacts with PGRN but not PGRN fragments. When we added SLPI in the GRN C and GRN E conditions, SLPI did not affect the neurotrophic ability of PGRN (Fig. 3.6C and D).

Previous experiments showed that neurite outgrowth increased after GRN C as well as GRN E treatment, and the increase in axon length and soma size was less than that by PGRN[31]. However, in contrast, we found that GRN C and E have an effect on axon growth extension than that by PGRN (Fig. 3.7A). Axon growth of MNs treated with GRN E significantly increased (341.24 ± 32 μm) and was about 2.2 times longer than that of control (Fig. 3.7B).

Our results demonstrate that PGRN were secreted from SC, which is a neurotrophic factor that enhances viability and axon growth of MNs. Interestingly, the viability of MNs decreased significantly at DIV 7 after culture as previously described. However, the PGRN fragments, GRN C and GRN E, were able to maintain the viability of MNs at DIV14.

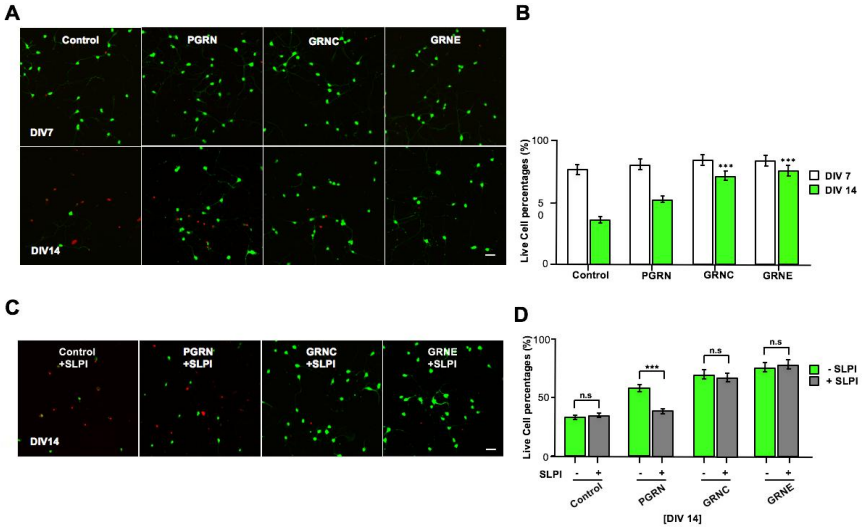

Figure 3.6. Protection of PGRN fragments against MNs' cell death. Representative images (A) and quantification (B) from calcein AM- PI stained MNs that were treated with PGRN, GRN C, GRN E (200 ng/mL/each protein) are shown for indicated time.

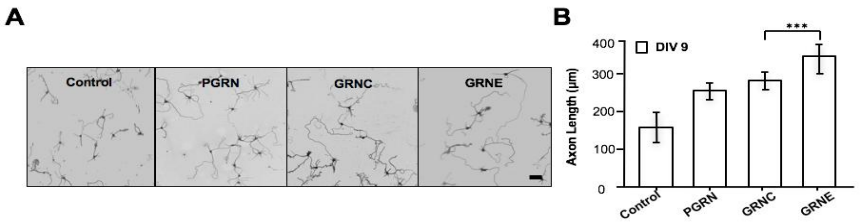

Figure 3.7. Promotion of axon growth of MNs by PGRN fragments. Representative images (A) and quantification results (B) of axon growth are shown.

Chapter IV.

Optogenetic Stimulation of Axon Growth of Motor Neuron.

1. Introduction

External stimulation has been known to have an effect on the survival and the growth of the neuron.[31,44,64] Among them, electrical stimulation (ES) has long been considered as a potential tool to stimulate axon regeneration of neurons in central and peripheral nervous systems.[65,66] When electrically stimulated with a low frequency DC pulse train for 1 hour, the axon regeneration of transected femoral nerve was greatly enhanced,[67] and it was mediated by the upregulation of BDNF and its receptor trkB.[36] It was also reported that a brief, low-frequency ES of transected sciatic nerve accelerated axon regeneration as well as myelination inside a silicon-rubber conduit interposed between two transected nerve stumps in animal model.[68] When cultured with SC *in*

vitro, on the other hand, the myelination of dorsal root ganglion (DRG) cells was reduced by ES with as low frequency as 0.1 Hz.[69] A recent in vitro model by Koppes *et al*.[70] demonstrated 7-fold increase of axon outgrowth by ES on DRG neurons encapsulated within carbon nanotubes (CNT)-collagen composite hydrogel. While presenting as a potential means to enhance neurite outgrowth and myelination for peripheral nerves, ES lacks a cell-type specificity, thus impeding the specific analysis of the underlying mechanism in particular for neuron-glia cell coculture models.

In Chapter IV, we introduce optogenetics as a stimulatory factor to promote axon growth in MN monoculture. Additionally, we investigate optically excitable MNs at low intensity, which can induce optical upregulation of proteins that is typically generated by signaling cascades.[71]

2. Material and Methods

A. Gene amplification and transfection

- *Gene amplification*

CatCh: ChR2(L132C)-YFP; vector: pAAV-CMV which has L132C mutation of humanized channelrhodopsin2 (ChR2) with H134R mutation fused EYFP was obtained from Addgene (Addgene Inc., USA) (Fig. 4.1).[72] To amplify pCatCh, plasmid was transformed into DH5∂ competent *E. coli* cells that is useful for recombinant DNA methods as it enables insert stability and promotes the quality of DNA purified from minipreps. Transformed bacterial cells were then cultured in LB medium (Sigma) containing ampicillin (1 mg/mL, 1:1000, Sigma) and incubated at 37°C for 18 hours. Bacterial pellet that harvested by spinning at 13000 rpm for 1 min, were resuspended in 250 μL resuspension solution containing RNaseA before cells were lysed in lysis buffer (400 mM NaOH and 2% SDS) and mixed gently by inverting 3 times. Lysed cells were then treated with neutralization buffer (5 M potassium acetate, pH 5.5) and centrifuged for 15 min to precipitate debris consists of bacterial DNA and protein. Cleared supernatants were transferred to a column carefully and centrifuged for 1 min at 13000 rpm. After washing the column twice with wash buffer containing 70% ethanol, distilled water (DW) was added in the column for elution of DNA.

- *Lipofectamine method*

To transfect MN with pCatCh-EYFP (Addgene) in MN regions of the device, the mixture of DNA (5 μg)-lipofectamine 2000 (Invitrogen) in serum-free MN medium was incubated for 30 min at room temperature. After incubation, DNA/ lipofectamine suspension was added in the MN chamber at DIV 2 for 1 day at 37°C incubator. The medium in the MN chamber was then changed with MN culture medium.[71]

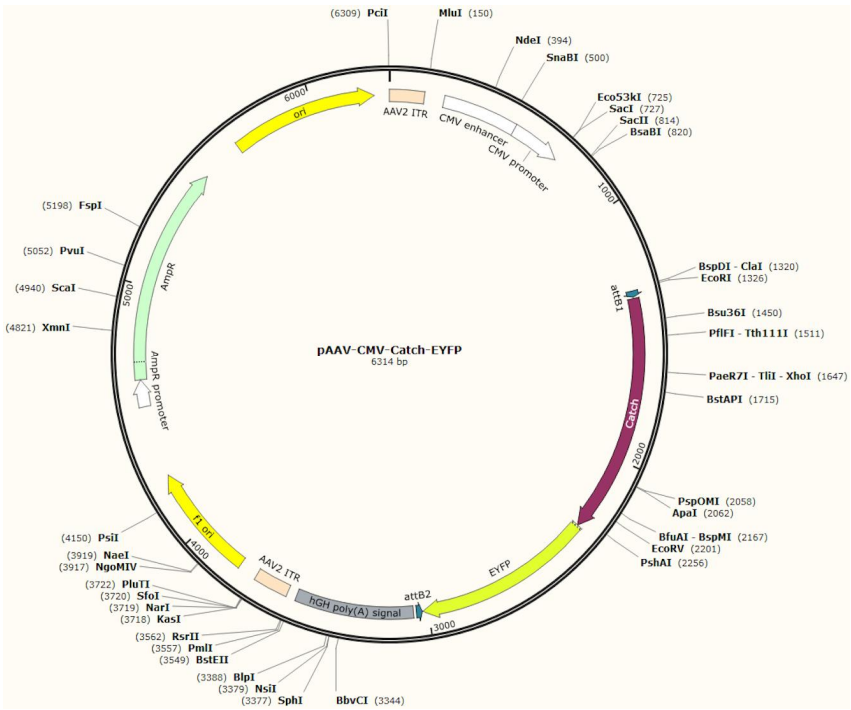

Figure 4.1. Gene map of pAAV-CMV-CatCh-EYFP. CatCh was constructed by L132C mutagenesis of humanized channelrhodopsin2 (ChR2) with H134R mutation fused EYFP (image reproduced by Dr. Eun Mi Hwang of Center for Functional Connectomes of Korea Institute of Science and Technology(KIST), Seoul, Korea).

B. Measurement of axon length

In Chapter IV, TuJ1-labeled MN in each group (control on/off) and both GFP and TuJ1 co-labeled MN in each group (Transfection on/off) were measured using ImageJ and quantified (50 axons/each group, N=5).

C. LED stimulation array

To transmit pulsed blue light to transfected MN, 24 blue light-emitting diodes were customized and modified as previously described (Fig.4.2).[44] Briefly, LEDs (473 nm wavelength) that were covered with 45 or 90 degrees lens (Eleparts) for uniformly illuminate to the target cells, and filtered out UV wavelength from UV protector film, were driven by power supply, DP832 series (Rigol technologies). The intensity of LEDs was yielded uniformly at an irradiance of 1 mW/mm^2 and delivered to optically-sensitive MN, as measured by an optical power and energy meter (Thorlabs). The duration of the light pulse was set to1 s, and the interval was set to 9 s.[71]

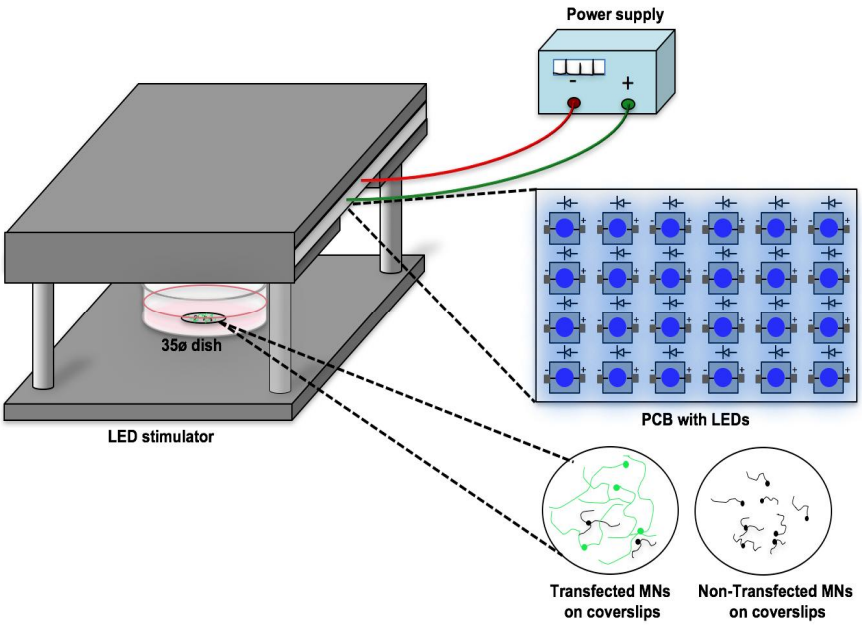

Figure 4.2. The schematic depiction of a custom LED array for optical stimulation.

D. ELISA analysis

The intracellular concentrations of cAMP and PKA in MN were measured using cAMP (Cayman Chemical, USA) and PKA kinase activity kit (Abcam, UK) according to the manufacturer's instructions. After 0, 1, 24, 48 hrs of optical stimulation, the cells were lysed in RIPA buffer (T&I) containing protease inhibitors Cocktail (Sigma) and centrifuged to remove cell debris for 5 min at 4˚C. After the total protein content of the cell lysate was measured by Bradford assay, the samples were loaded onto the ELISA plates. The samples for cAMP analysis needed to be acetylated to amplify the signal level before being loaded onto the plate. The optical absorbances for cAMP and PKA were measured using microplate reader (Thermo) at 450 nm, and were quantitated against the respective standard curves.

3. Results

A. Gene transfection using lipofectamine and transfection efficiency

We used a special ChR2 variant to excite cells at lower intensity. Kleinlogel *et al.*[72] reported a new ChR2 variant; CatCh that is an ultra light-sensitive Ca^{2+} permeable ChR2 variant than that of wild- type ChR2 allowing accelerated response time, and is expressed on the membrane, not in cytosol. We measured the transfection efficiency of MNs after transfection of pCatCh using lipofectamine reagents (Fig. 4.3A) and quantified the transfection efficiency as the ratio of counted MN, which co-labeled with GFP and DAPI, over MNs stained DAPI only (Fig. 4.3B). We confirmed that about 75%~80% cell bodies were co-immunostained GFP and DAPI, compared to MNs stained DAPI only (Fig 4.3B).

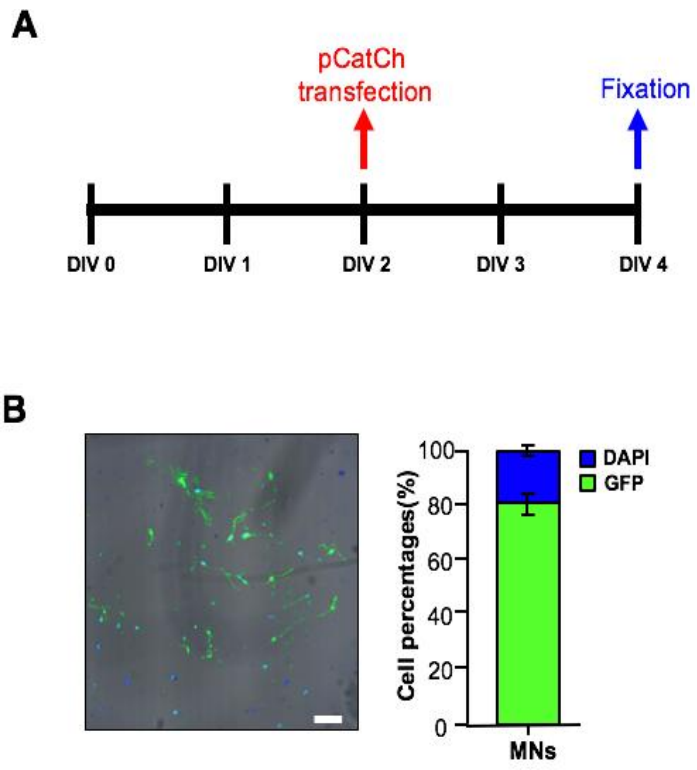

Figure 4.3. CatCh-expression in MNs. (A) Schematic procedure of preparation of MNs that were transfected with pCatCh using lipofectamine reagent at DIV 2, and efficiency of pCatCh transfection was analyzed by immunocytochemistry at DIV 4. (B) Representative images (left panel) and quantitative results (right panel) are shown. Scale bar, 100 μm; n=3, three random regions.

B. Phototoxicity and MN viability

MNs are more sensitive than other peripheral neurons such as DRGs that isolated from transgenic mouse expressing ChR2 can be optically sensitized at 5~6 mW intensity using optical stimulation.[44] However, MNs is not. MN monocultures are very difficult to maintain for a long time[17, 45, 75, 76] and are susceptible to external environment such as light, temperature and CO_2 conditions. We next assessed the MNs viability under different light intensity (1 mW~ 8 mW/mm^2) at DIV 4, and measured it by using calcein-AM and PI assays kit at DIV 5 (Fig. 4.4A). We identified that MN steadily survived under light stimulation compared to non-stimulated MNs (Fig. 4.4B). The MN viability was quantified as shown in Figure 4.4C. MN viability was maintained at 3 mW or less intensity and was significantly decreased at 5 mW of more intensity. However, MN viability (73%) at 3 mW intensity was slightly reduced compared to non-stimulated MNs, and the ratio of MN viability at DIV 7, was similar to a previous report.[45] Lower light intensity (1 mW/mm^2) was chosen to excite MN, consistent with the threshold for ChR2- facilitated neural excitation. No significant difference between control and 0 mW was observed.

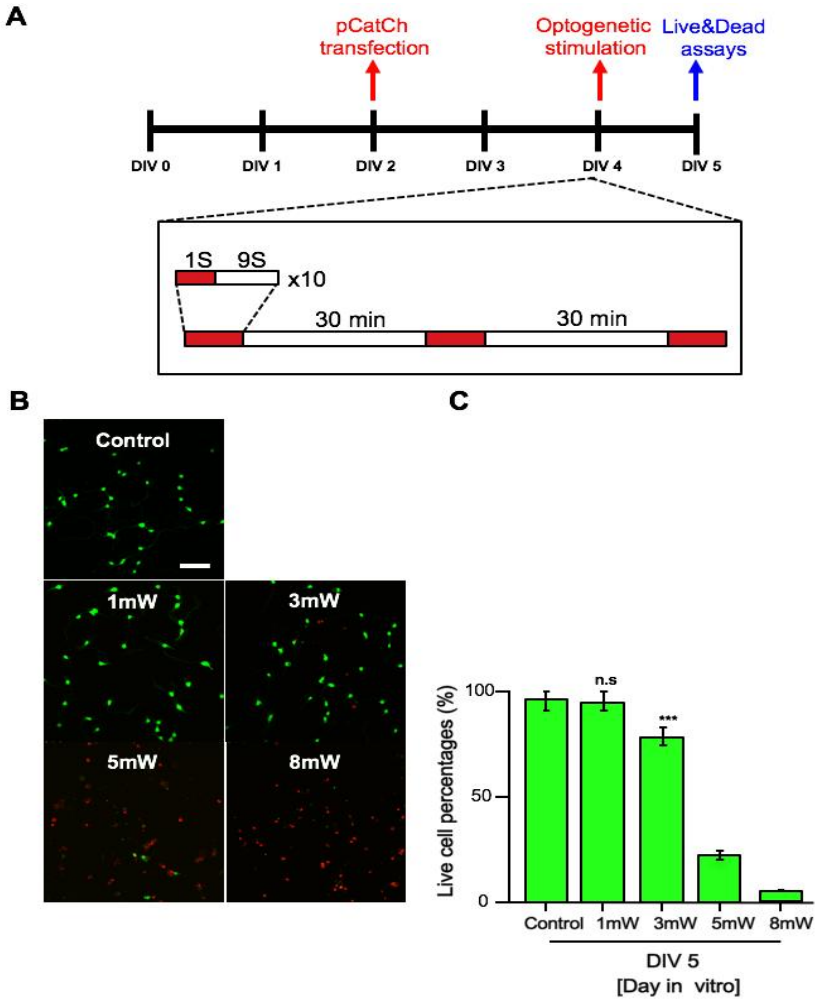

Figure 4.4. Cell viability by optical stimulation at different intensities. (A) Temporal schematic of optogenetic stimulation of 2-D MN culture. The inlet shows the blue light-stimulation protocol of ON for 1 s and OFF for 9 s, repeated ten times over the period of 100 s. (B) Viability of transfected MN by optogenetic stimulation was measured by double-staining with calcein-AM and propidium iodide (PI) at 0, 1, 4, 5, 8 mW intensities, as indicated (n=3). Scale bar, 100 μm.

C. Axon growth by optogenetic stimulation

We next asked if axon growth of MN was also influenced by optical stimulation as a means to promote axon length of other neurons as previously described.[44]

To investigate the effect of optical stimulation on axon growth of transfected MNs, we examined optically stimulated CatCh-MNs, as compared to unstimulated CatCh-MNs, stimulated WT-MNs, and unstimulated WT-MNs (Fig. 4.5B). The optical stimulation was conducted using custom-built setup designed to provide uniform stimulation 10 cycles of 1 s ON and 9 s OFF. MNs were stimulated three times every 30 min (473 nm wavelength, 1 mW/mm^2). Consistent with previous works,[44,71] axon growth of optically sensitive CatCh-MNs significantly increased by 2.5 fold than other groups (WT_ON, 145.6±18.3 μm; WT_OFF, 142±14.7 μm; CatCh_ON, 388.1±82.7 μm; and CatCh_OFF, 182.3±29.6 μm). We measured and confirmed axon growth of GFP-labeled MNs (Fig. 4.5B) and quantified it (Fig 4.7B, right panel). Taken together, we identified that the optically evoked neural activity promotes axon growth of MNs.

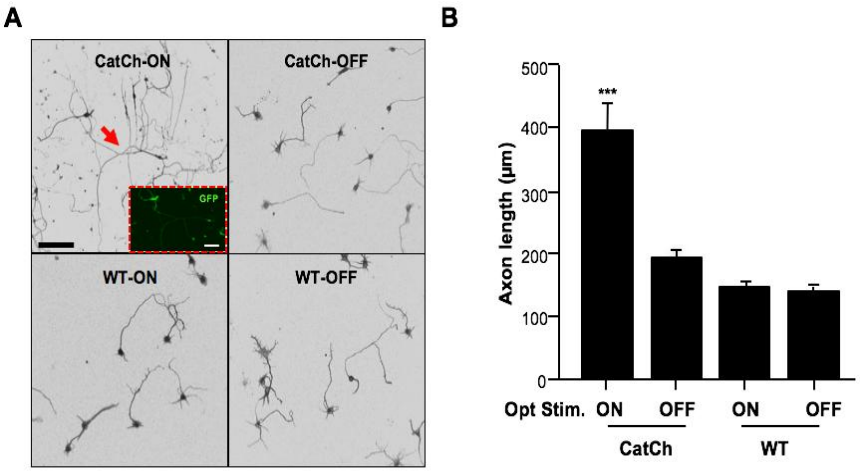

Figure 4.5. Axon growth of CatCh-MN by optogenetic stimulation. (A) Schematic procedure of sample preparation to analyze axon length after MNs were transfected and stimulated by blue light before fixation for immunostaining. (B) CatCh-MNs treated with blue light were immunostained with TuJ1 to visualize the axon at DIV 5. Arrow (red) indicates GFP co-labeled MN, magnified in the red dotted box inset. Axon length of MNs was measured using ImageJ software, and compared between control MN with or without optical stimulation and CatCh-MN with or without optical stimulation. Each bar represents mean ± S.E. value. n=5, 50 axons/each group; ***$p < 0.001$; Scale bar, 100 μm.

D. Optogenetic upregulation of intracellular cAMP and PKA

Previous studies have reported that elevated intracellular cAMP levels are sufficient to induce axon outgrowth and branching as well as neuronal viability.[64,78-81] Thus, we next examined whether optically induced activity triggered axon growth-related cell signaling. Intracellular cAMP and PKA levels of MNs at 1, 6, 24, 48 hours after optical stimulation were measured in comparison with control. As expected, optically stimulated CatCh-MNs showed upregulated intracellular cAMP as well as PKA expression levels after stimulation, whereas cAMP and PKA expression levels of optical stimulated WT-MNs were low (Figs. 4.6A and B). Furthermore, our results demonstrate that the PKA downstream of cAMP regulates axon extension after optical stimulation as previously described.[78] Schematic representation of the mechanism by which lower intensity of optical stimulation stimulates axonal extension is shown in Fig. 1.4. Optical stimulation upregulates intracellular cAMP via PKA, which might lead to transcription and translation of axon growth-associated factors.

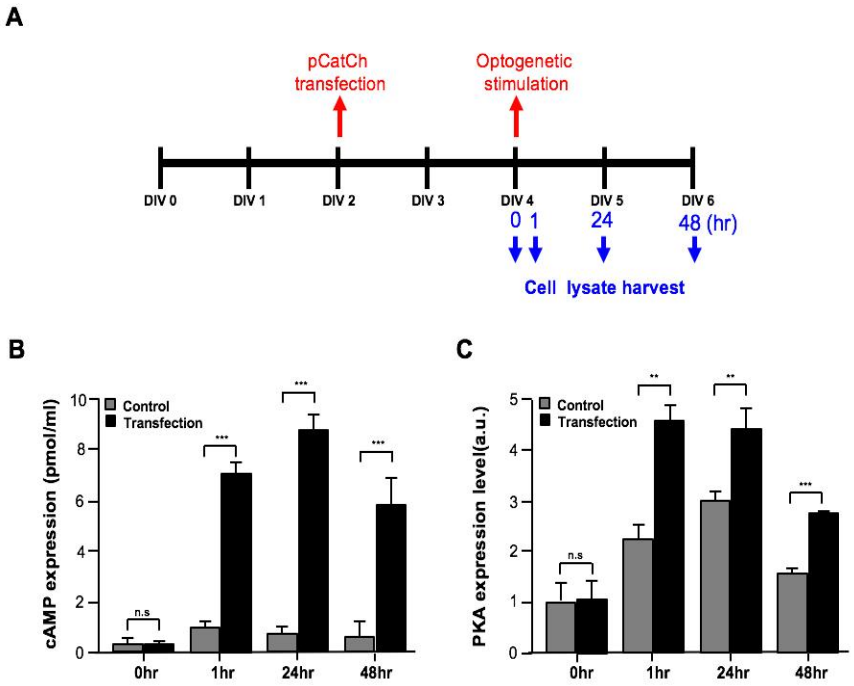

Figure 4.6. Intracellular level of cAMP (B) and PKA (C) expression in 2-D MN culture under optogenetic stimulation. (A) Schematic procedure of sample preparation to analyze protein expression after optogenetic stimulation. Intracellular levels of cAMP and PKA were measured using ELISA at 0, 1, 24, and 48 hrs after optical stimulation. As expected, cAMP and PKA expression in CatCh-MN were upregulated, as compared to those of WT-MN, as early as 1 hr post-stimulation. Each bar represents mean ± S.E. value. n=3; $^{**}p < 0.01$, $^{***}p < 0.001$.

Chapter V.

3-D Coculture Model of MN-SC in Microfluidic Biochip

1. Introduction

With recent advances in micro-fabrication technology using bio-friendly polymers, such as polydimethylsiloxane (PDMS), researchers have introduced various microfluidic platforms, which allow *in vitro* studies on certain controlled characteristics of axon growth, injury and regeneration of neurons with or without glia cells. Jeon and his colleagues[14,19,22] presented a microfluidic culture chamber in which axon compartment can be separated from cell soma and studied the outgrowth of neuronal axon independent of neuronal somata. More recently, Park *et al.*[20,21] introduced a multi-compartmentalized microfluidic culture device for coculture of cortical neurons and oligodendrocytes to study myelination process of CNS neurons. Kamm and his colleagues[82,83]

introduced a neuromuscular junction model on a compartmentalized microfluidic device, which consisted of myoblast-derived muscle cells and embryonic stem cell-derived MNs.

In Chapter V, a 3-D MN-SC coculture model with microfluidic chambers, which allows a separation between MN and SC cultures and yet maintains interactions between the two cell types. We also have utilized optogenetics to achieve a cell-type specific emulation of ES, similar to a previous work by Park *et al.*[44] By incorporating genetically encoded opsin for cation channels into neurons, optogenetics allows optical stimulation of the cell to activate action potentials in the optogenetically transfected neurons.[77] In our study, we used CatCh, an ultra-light sensitive Ca^{2+} permeable variant of channelrhodopsin-2,[72] which allows a low light activation of action potentials in neurons. Using the 3-D hydrogel microfluidic chamber, we also investigated the effects of coenzyme Q10 on the MN myelination, which previously demonstrated an ability to accelerate myelination process in 2-D MN-SC coculture.[45]

2. Materials and Methods

A. Fabrication of microfluidic biochip

The master mold was fabricated on silicon wafer by using photolithography with SU-8, the negative photoresist (MicroChem, USA). After fabricating master mold, polydimethylsiloxane (Sylgard 184, Dow Corning, USA) made of a 10 : 1 (w/w) mixture of PDMS base and curing agent was poured on the master mold and cured for 30 min in 95˚C. The cured PDMS was peeled off from the master mold. Hydrogel injection ports and the reservoirs for cell culture medium were punched out with biopsy punches. The PDMS device was permanently adhered to a sterilized glass coverslip by air plasma. After bonding, the PDMS device was cured in 85˚C dry oven for a week to restore hydrophobicity. The PDMS device was sterilized by UV irradiation before experiment.

B. MN-SC coculture on biochips

3-D MN-SC coculture was first carried out in a mixture of collagen type I and Matrigel (1:1) in the microchannel regions of the microfluidic device. The gel was then incubated to polymerize for 20 min at room temperature and reservoirs were filled with culture medium, and the medium was drained from the opposite reservoir by suction to produce

hydrophilic surfaces in all medium channels. The devices filled with gel were tilted to align the gel at 90 degrees angle for 16 hrs and kept in 37°C incubator prior to cell seeding. SC suspensions ($3x10^6$ cells/mL) were injected into the right reservoir of the microfluidic device, and the device was tilted to allow cells to adhere near gel surface for 30 min at 90 degrees angle. After 24 hrs, MN suspensions ($2x10^6$ cells/mL) were again placed in the opposite reservoir of the device and tilted at 90 degrees angle until the attachment of MN to the gel surface. Coculture cells in the device were cultured with neurobasal medium consisting of 2~10% HS, B27 supplement, 0.5 mM L-gln, 0.5~1 mM β-mercaptoethanol, 0.5 μM forskolin, 1 mg/mL bovine pituitary extract, 10 ng/mL BDNF) for 7 days, after which 25~ 0 μg/mL of ascorbic acid (Sigma) was added for the subsequent culture as previously described.[45] Medium was replenished four times a week.

C. Quantitative analysis of pre-myelinating and myelinating Schwann cells

For MBP or TuJ1 expression level analysis, each individual fluorescence image under the same condition of confocal microscopy was converted to a grayscale image. The integrated surface plot of fluorescence intensity (i.e., integrated intensity plot) associated with each protein was then acquired over the entire gel region in the biochip using ImageJ and

quantified. The samples were analyzed at DIV10, which corresponds to a pre-myelinating phase and DIV20, which corresponds to a myelinating phase, respectively (n=3).

D. Statistical analysis

Average data were shown as mean ± standard error, and the comparison between different groups was performed by using repeated measures analysis of variance (ANOVA). Statistical significance was set at a value of $*p < 0.05$, $**p < 0.01$, $***p < 0.001$.

3. Results

A. Establishment of 3-D MN-SC coculture model in the biochips

We used a microfluidic biochip that consisted of three distinct microfluidic channels: one channel for MN culture, another for SC culture, and a central channel interposed between the two cell-culture channels. The central channel was filled with a mixture gel of collagen-Matrigel that separated the MN and SC culture, and provided a 3-D microenvironment for axon growth and myelination of MN (Fig. 5.1). To form 3-D MN-SC coculture model, we received the microfluidic biochips from NL Jeon's laboratory at the Seoul National University, and carried out the procedure according to the Bang *et al*.[22] study. Briefly, the microfluidic biochips have composed of three distinct channels including MNs, SCs, and gel channels (Fig. 5.1A). In particular, gel channels of these biochips are useful to extend axons regularly toward opposite direction. The mixture gel (collagen:Matrigel, 1:1)-filled gel channel in the biochips was tilted at 90 degrees angle to induce the hydrostatic pressure generated by the medium added in the reservoirs. This allowed a uniform alignment in polymerizing gels (Fig. 5.1B).

After gel loading, SCs, which were suspended in 50 μL of SC medium, were added to the microfluidic biochips. The hydrostatic pressure that

was induced in biochips, tilted at 90 degrees, generated a continuous fluid flow that distributed SCs to attach to the surface of gel channel. MNs were also loaded in other reservoirs after SC seeding, and the biochips were tilted at 90 degrees for 30 min to allow MNs to adhere near the surface of the gel channel. Prior to cell loading, alignment of the mixture gel in the gel channel supported a more uniform distribution of cells, which induced uniform axon growth towards the opposite channel, and generated migration of SCs evenly (Fig. 5.2). Furthermore, the structure of gel-filled channel in the microfluidic biochips provided a culture of distinct cell populations and allowed the transfection of MNs only. pCatCh-EYFP were transfected to MNs using lipofectamine reagent in the MN reservoirs before axons of MN interacted with SCs, and expression of pCatCh was confined to MNs in the MN reservoirs that received the pCatCh transfection. GFP expression was seen in MNs in MN channel, but not other SC channel (Fig. 5.2, top panel). On DIV 4, transfected MNs were optically stimulated to trigger axon growth, and treated with coenzyme Q10 (Co-Q10) to activate the myelin process. We examine the detailed myelin stages at DIV 10 and 20.

A

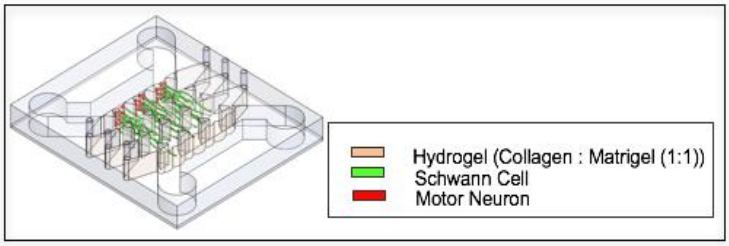

B

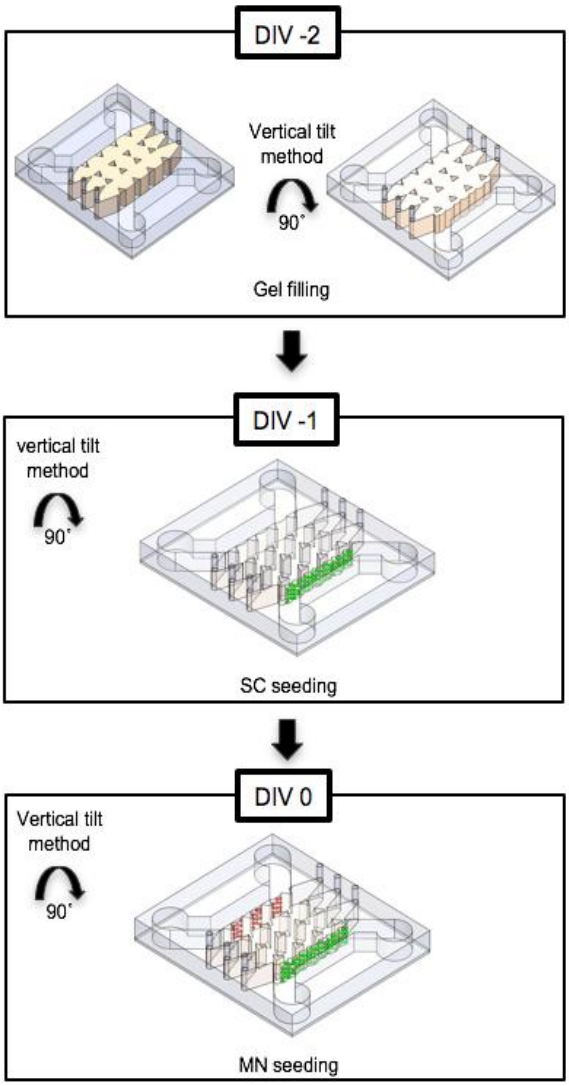

Figure 5.1. 3-D MN-SC coculture model on microfluidic biochip; (A) Microfluidic biochip consists of five distinct channels separated by four micropillar arrays; three central channels for hydrogel formation, one channel for SC culture, and one channel for MN culture. (B) On DIV-2, three central channels were filled with a 1:1 mixture of collagen and Matrigel at 4˚C, and a hydrostatic pressure created by 90˚ vertical tilt method was applied onto the mixture gel during gelation process in 37˚C incubator in order to create a patterned cross-linking density distribution in the hydrogel. SC and MN were then seeded and attached using vertical tilt method onto the gel surface in the respective cell culture channel on DIV-1 and DIV0, respectively.

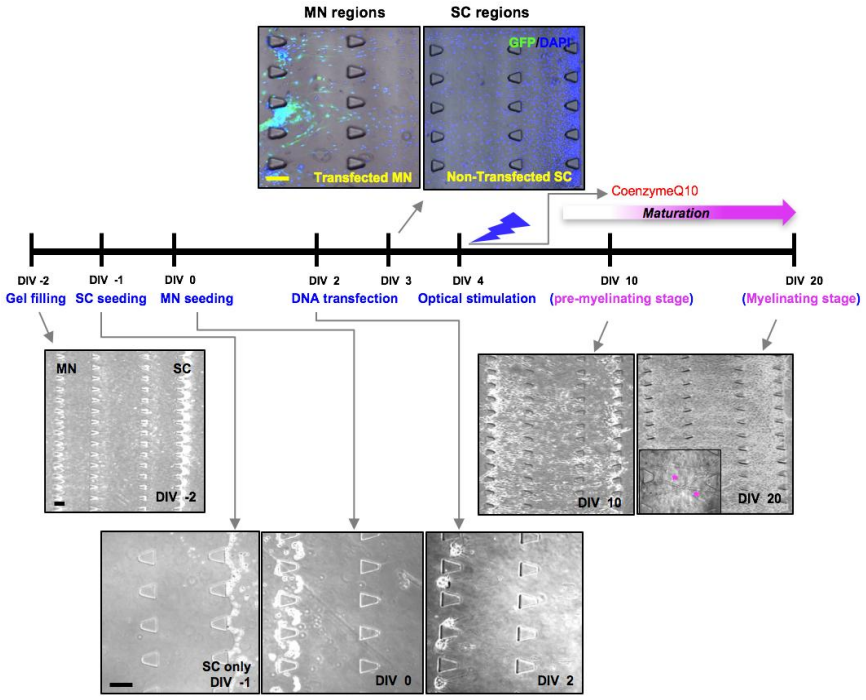

Figure 5.2. Temporal flowchart describing the protocols of 3-D MN-SC coculture study. Microscopic images of 3-D MN-SC coculture biochip are shown at different time points. At DIV 2, the gel channel was filled with a collagen-Matrigel (1:1) mixture. SCs and MNs were seeded through cell-seeding reservoirs at DIV 1 and DIV 0, respectively. On the second day after MN seeding (DIV 2), pCatCh (5 μg) with lipofectamine was loaded into MN channel. Fluorescent microscopic image at DIV 3 confirmed CatCh-transfected MNs. Note in the microscopic image that CatCh transfection was visible only in the MN region, not in the SC region. The MN-SC coculture biochip was examined for MBP-expression at DIV 10 (pre-myelinating stage) and at DIV 20 (myelinating stage), respectively. Scale bar, 100 μm.

B. Axon growth by optical stimulation

We first examined the axon growth on 3-D microfluidic biochip in which axons grow uniformly regularly towards the opposite channel, and that can serve as quantitative analysis for growing axons. We observed the effect of optical stimulation on the axons of MN, extended into the gel channel of biochip, as assessed by immunocytochemistry (Fig. 5.3, left panel). At DIV 5, optically excitable CatCh-MN axons significantly increased (694.4 ± 17.7 μm) and the length was 2.1-fold longer than that of control (333.8 ± 17.1 μm) (Fig. 5.3, right panel). We confirmed the effect of optical stimulation on axon growth in both 2-D and 3-D formation of MNs.

In MN-SC 3-D model, we examined the axon growth in each group using immunocytochemistry, and quantified it at DIV10 and 20. However, optogenetic stimulation did not affect axon growth in MN-SC coculture model. At DIV 10, axon growth of all groups were already elongated to the opposite channel of SCs, and there was no difference in axon growth in each group analyzed by the pixel intensity of TuJ1 stained-axons (Control, 630.2 ±14 μm; Optstim., 672.3 ± 8 μm; Co-Q10, 624.2 ± 23.6 μm; Optstim.+Co-Q10, 696.9 ± 7.4 μm). In addition, at DIV20, we did not observe the benefit of optogenetic stimulation in 2-D

MN culture (Control, 694.2 ± 5 μm; Optstim., 704.3 ± 14.5 μm; Co-Q10, 690.1 ± 21.8 μm; Optstim.+Co-Q10, 744.9 ± 15.9 μm).

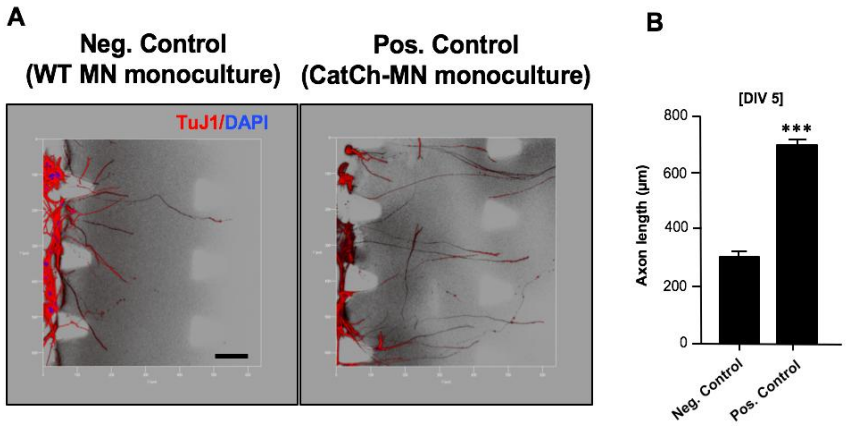

Figure 5.3. Axon growth of MN monoculture in 3-D microfluidic biochip with (CatCh-MN, positive control) or without (wild type MN, negative control) optical stimulation. (A) TuJ1 stained images of MN axons for negative control and positive control on DIV 5. (Scale bar, 100 mm) (B) The length of TuJ1-stained axons was quantified using ImageJ software. CatCh-MN under optical stimulation produced significantly increased axon length, as compared to WT-MN without optical stimulation. Error bars indicate S.E. (n=3, total 30 axons)

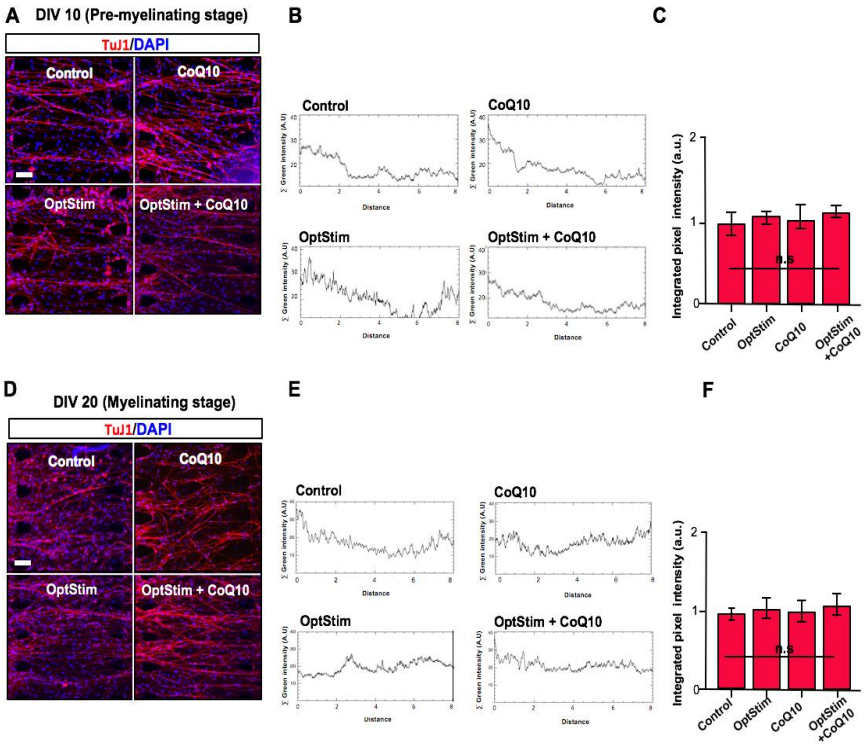

Figure 5.4. Effects of optogenetic stimulation and/or Co-Q10 treatment on axon growth of MN in 3-D MN-SC coculture model. The pixel intensity of TuJ1-stained axons of each group was measured by ImageJ (A-C) on DIV10, (D-F) on DIV20. Representative confocal images (A and D) and the intensity distribution (B and E) of TuJ1 expression in MN-SC coculture biochip, in which TuJ1 and DAPI were shown in red and blue, respectively. (C and E) Quantitative results of the integrated pixel intensity of MBP expression. No significant differences were found by One Way ANOVA. Each bar represents mean ± S.E. value (n=3, 5 random regions).

C. Two distinct stages of myelination in biochips

SCs in the PNS have significant functions to support neurons including dorsal-root ganglia (DRGs) and MNs, which express neurotrophic factors such as nerve growth factor (NGF),[55] brain- derived neurotrophic factor (BDNF),[58] and ciliary neurotrophic factor (CNTF)[26] to promote axon growth and viability of neurons. Furthermore, SCs are particularly important in myelination of axons of neurons in PNS, wherein wrapping of neurons by SCs increases the speed at which impulses are conducted. In our study, we next examined the myelin process in the microfluidic biochip to validate our microfluidic biochips as a 3-D coculture platform. We identified distinct stages of MBP expression at DIV 10 (Figs. 5.5A-C) and DIV 20 (Figs. 5.5D-F). We classified the myelin process, which could be distinguished on basis of MBP expression pattern as described previously.[45] We identified that in the pre-myelinating stage, coculture model with Co-Q10 extensively expressed MBP in SCs, whereas we did not detect MBP expression in coculture model without Co-Q10 at DIV10 (Figs. 5.5A and B).

However, in myelinating stages, MBP expression by SCs eventually became highly localized around axons similarly in all group of the microfluidic biochips (Fig. 5.5D and E, and Fig. 5.6). We observed that myelin sheaths of 3-D form were aligned along the MN axons, which

mimicked the in-vivo condition in MN-SC coculture model (Fig. 5.6, yellow dotted boxed/each group). In addition, we calculated the integrated pixel intensity of MBP expression at distinct two stages quantitatively (Fig. 5.6C and F). We confirmed that Co-Q10 is a significant activator that promotes MBP expression rapidly at DIV10, which can be useful to stimulate SC differentiation against myelin process in SC development.

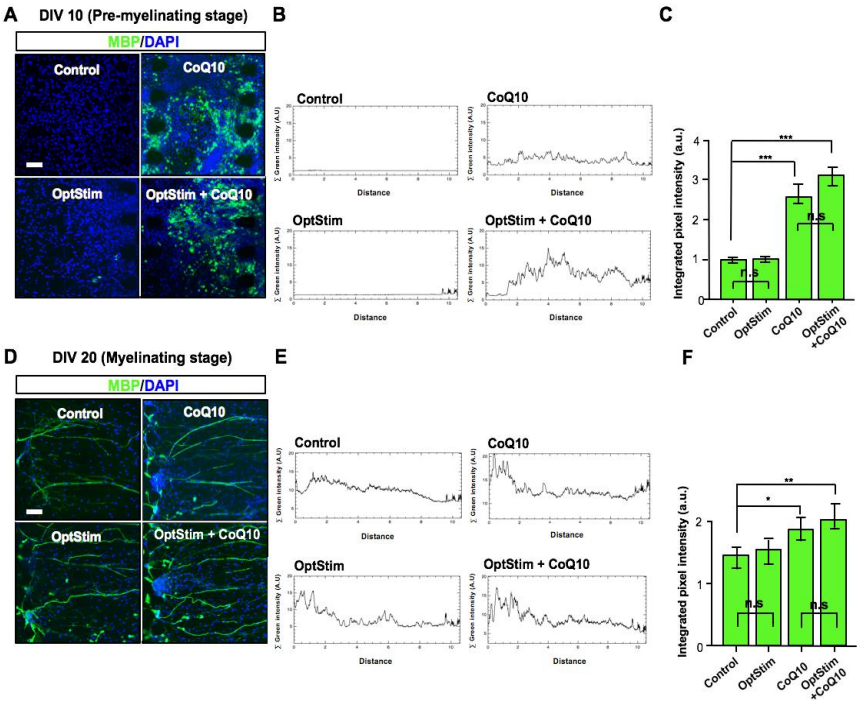

Figure 5.5. Effects of optogenetic stimulation and/or Co-Q10 treatment on MBP expression of MN in 3-D MN-SC coculture model. Representative confocal images (A and D) and the intensity distribution (B and E) of MBP expression of MN-SC coculture biochip, in which MBP and DAPI are shown in green and blue, respectively. Note that MBP expression was widespread in the culture in pre-myelinating stage (A), but aligned tightly along the MN axons in myelinating stage (D). Quantitative results of the integrated pixel intensity of MBP expression were presented in (C) and (F). Each bar represents mean ± S.E. value. (n=3, 5 random regions; ***$p < 0.001$; Scale bar, 100 μm.

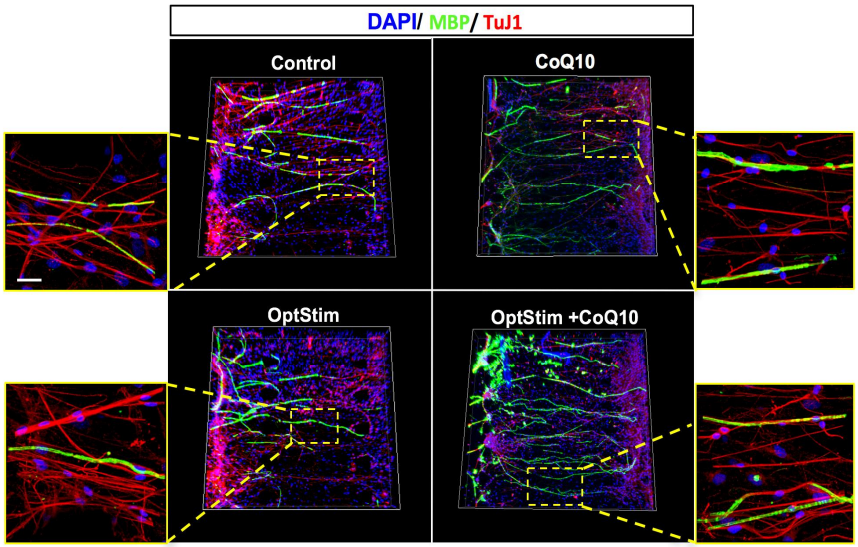

Figure 5.6. Representative 3-D reconstruction image of MN-SC coculture on the biochip. The culture was immunostained with TuJ1 (red), MBP (green) and DAPI (blue) (control, OptStim, Co-Q10, and OptStim + Co-Q10). All biochips showed abundant MBP expression, and highly myelinated axons were visible in high magnification images (yellow dot boxes/each group). Scale bar, 25 μm.

Chapter VI.

Discussion and Conclusion

1. Discussion

Several *in vitro* models have been previously developed to study the cellular and molecular mechanisms involved in the myelination process. Sensory neurons from dorsal root ganglia[12,13,84,85] and retinal ganglia[86] have been cocultured with SCs to induce the formation of myelin sheath *in vitro*. Several *in vitro* models for MN culture have also been introduced,[16,17,19,27,47] and the findings from these studies have confirmed that addition of exogenous neurotrophic supplements and/or a coculture with SCs or fibroblasts was critical for the survival and neurite outgrowth of MNs cultured *in vitro*. MN cultures treated with astrocyte-conditioned medium[87] or insulin-like growth factor-1[27] could specifically enhance the extent and rate of axonal outgrowth from murine

corticospinal MNs. However, to the best of our knowledge, no culture method to date has recapitulated the myelination process of MN by SCs *in vitro*. Moreover, previous studies have attempted to culture MNs by using NycoPrep™, OptiPrep™, or immunopanning dishes, but the purified MNs frequently failed to survive long-term.[17,47,88] In this study, we have aimed at constructing a MN-SC coculture system to model both the axon outgrowth and the myelination process of MN.

Here, we confirmed that SCs play an essential role in increasing the viability and promoting axonal outgrowth of MNs. Consistent with our results, several groups have reported that SCs enhance long-term viability of peripheral neurons and protect the axonal integrity. Meyer zu Horste *et al.*[89] reported that dysfunction of SCs leads to peripheral neuropathies, and Viader *et al.*[90] found that mitochondrial function in SCs is essential not only for neuronal survival but also for normal function of peripheral nerves. Similarly, glial cells have been shown to play a vital role for the growth and stability of developing synaptic structure as well as for proper functioning of neuromuscular junction.[91] With regard to nerve injury, it is well documented that SCs play a role in promoting recovery of the injured PNS by providing beneficial environment to the injured neurons.[92,93] SCs de-differentiate, proliferate, and form Bands of Büngner at the injury site, by which they guide the regrowth of the proximal axons towards the target.[94] Our results, along

with the previous reports, support the notion that SCs play an essential role in controlling the viability, axon growth, and perhaps the functions of MNs.

In addition, we confirmed neurotrophic effects of protein secreted from SCs by using transwell that enabled separation between MNs and SCs culture in the same medium, which consequently promoted the viability and axon growth of MNs, and inhibited the effects by adding SLPI. In particular, we identified the loss of about 46% by SLPI on MNs viability at DIV 14 (Fig. 3.1), suggesting that PGRN are necessary to maintain MN survival and the remaining viability of MNs might be influenced by other neurotrophic factors secreted from SCs as previously described.[23,25,58]

PGRN has been recently demonstrated to play a key role in several fields, including cancer models such as bladder,[95] breast, hepatocellular carcinomas, and neurodegenerative disease such as FTLD and ALS.[96] Furthermore, several laboratories have demonstrated a critical role of PGRN derived from specific types of cells, including adipose-derived stem cells[97] and human mesothelioma cells.[33] PGRN secreted from cells not only induces the differentiation of retinal precursor cells to photoreceptor cells[97] but also promotes supernatant-induced tube formation[33] when tissue is damaged. These results are consistent with our

finding that PGRN is a secreted growth factor derived from SCs and serve as regulator of MN growth.

Notably, we confirmed the effect of PGRN on MN viability wherein PGRN and GRN fragments sustained MNs without SCs for at least 2 weeks (Fig. 3.6). We also found that MNs are more vulnerable to attack by environment, and MNs viability could not prolong after day 10 in MNs monoculture. These findings suggest that PGRN is a powerful neurotrophic factor for maintenance of MN viability,[34,35] and might be useful a biochemical candidate for therapeutic trial in disease model of motor neuron with ALS and FTLD.[96]

In addition, other than the neurotrophic factors, external stimulation has been known to have an effect on axon growth in developing neurons.[37,44] Here, we used optogenetics to induce axon growth of MNs, which takes advantages of high conductance and the fast kinetics of optogene that allows activation of axon growth-related proteins. Unlike electrical stimulation, optogenetic stimulation can be genetically targeted to allow exploring of specific neurons, avoiding the simultaneous activation of multiple cell types. However, rapid cell death of MNs occurs when optically sensitive MNs are excited by LED stimulator at intensity of 5 mW/mm^2 or above, while other types of neurons[44] were activated at intensity of 5~7 mw/mm^2. Therefore, CatCh is prerequisite for researching optical activity of MNs, which is ~70 fold more light

sensitive than wild type.[72] When optically sensitive CatCh-MNs are stimulated at intensity of low level (1 mW/mm^2 or under), axon growth of MNs exhibited a ~2.6-fold increase in length compared to WT MNs. Furthermore, these results have demonstrated elevated cAMP and PKA expression level after stimulation. Consistent with our previous ELISA results, Aglah *et. al.*[78] reported that PKA, downstream of cAMP, controls neurite outgrowth and elongation of MNs on a permissive substrate.

Our culture enables monitoring of the pre-myelinating and myelinating stages of SCs *in vitro*. Signals released from SCs are critical for myelination of peripheral nerve fibers.[48] NRG1 (neuregulin) in the axonal membrane is essential for initiating the myelination process by binding to ErbB (erythroblastic leukemia viral oncogene homolog) family receptors expressed in SCs, and SC-derived signals are thought to primarily control the wrapping process of myelin around the axon. Among them, Krox20/Egr2 (early growth response-2), which functions downstream of Sox10 (SRY-related HMGbox-10) and is activated by Oct6 (octamer-binding transcription factor-6), is essential for activating a number of myelin genes and maintaining the myelinated state by blocking inhibitors of myelination. Our results in Fig. 2.7 show that Sox10 expression at DIV 7 preceded MBP expression, which was observed at DIV 10. The results in Fig. 2.8 also show a gradual increase of Krox20 first detected on DIV 7, followed by a strong expression at a

later stage (DIV 21). At later stages, MBP was highly localized along the axon fibers (Fig. 2.9). Our findings are consistent with the well-documented hierarchy of SC transcription factors controlling myelination (reviewed by Pereira *et al.*[48]). In our culture, we were able to confirm the sequential process of myelination, which was initiated by migration of SCs toward axons, followed by further differentiation of SCs, as evidenced by increased expression of MBP. Finally, SCs wrapped around axons, leading to the formation of thick myelin sheaths.

In the present study, we examined the efficacy of two candidate drugs, which might promote myelination of nerve fibers. We tested the effect of riluzole, a drug that is thought to protect neurons by decreasing the level of glutamate, and approved by FDA and clinically used for the treatment of ALS.[98] We also tested the effect of Co-Q10, a vitamin-like antioxidant substance that enhances ATP production in mitochondria. We found that while riluzole had no significant effect on myelination of MN axon fiber, Co-Q10 facilitated MBP expression and enhanced myelination. Lack of positive effect of riluzole confirmed in our study could be explained within the context of the controversy about the efficacy of riluzole treatment of ALS.[99] SCs treated with Co-Q10 expressed MBP at an earlier stage (DIV 7), implying that Co-Q10 might accelerate myelination of nerve fibers. MNs seem to have higher energy demand and metabolic rate due to their increased mitochondrial activity in

comparison to other neurons.[46] The stimulating effect of Co-Q10 found in our study could be due to its ATP synthesizing ability as electron carriers[100] or the antioxidant nature of Co-Q10,[101,102] or a combination of both. The exact mechanism and efficacy of Co-Q10 warrants further studies.

In the last chapter, we discussed a 3-D MN-SC coculture model in microfluidic devices that are helpful to allow uniform directional growth of axons by regularly aligned pores in gel. These chips have a fascinating advantage that enables quantitative analysis of axon growth and detailed examination of MN-SC interaction in 3-D formation. We also applied various factors on to the model for promotion of the axon generation and myelination. However, when MNs were cocultured with SCs, we did not observe optogenetic effects on axon growth of MNs while MNs were only cultured without SCs. Previous studies reported that SC is a powerful source, which can maintain the viability of MNs for more than 3 weeks and increase axon growth, about 4 fold times more in length than MN monoculture without SCs.[45] Because MN axons were strongly elongated by SCs already before anticipating the growth effect by optogenetic stimulation, we did not observe the dramatic effect of optogenetic stimulation on MN-SC coculture (Fig. 5.4). However, the result (Fig. 5.3), where MN axons without SCs in microfluidic biochips were promoted by optogenetic stimulation is consistent with 2-D model

as previously mentioned in chapter Ⅲ. In addition, we expected to promote myelin process by optogenetic stimulation that has the same principle as electrical stimulation for inducing the action potential in neurons. Similar to axon growth induced by electrical stimulation,[10,36,78] we identified increase in axon length by optogenetic stimulation through elevated cAMP and PKA expression level compared with that of control (Fig. 4.8).

In addition, we also examined the other functions of optogenetic stimulation, that is myelination. But our studies did not show the promotion of myelin process with optogenetic stimulation. However, regulation of myelination by electrical stimulation remains controversial. Several laboratories reported[103] that impulse activity by electrical stimulation might have a critical influence on myelination in CNS and PNS, but there are some differences between the published reports. Zalc group[103] claimed that impulse activity in axons is necessary for initiating myelination in CNS. They reported that oligodendrocytes, which are the glial cells of CNS were proliferated and differentiated by electrical stimulation in the absence of neurons *in vitro*, which can wrap around themselves to form myelin-like formations or adhere to carbon fibers to promote myelination. In contrast, Fields group[103] reported that DRGs in PNS did not influence and inhibit myelination by frequency-specific

effects of electrical stimulation, wherein low frequency stimulation (0.1 Hz) could induce decrease in the amount of LI, one of the neuronal cell adhesion molecules (CAMs) in the axonal membrane, that have a critical role in initiation of myelination. However, other frequencies of electrical stimulation (1 Hz) induced myelination in DRGs, but these impulse activity influencing myelination might differ in different types of neurons with different firing patterns as well as different stages of myelination, including premyelinating SCs and myelinating SCs in development. Furthermore, the number of SCs was not different in electrically stimulated or unstimulated cultures unlike oligodendrocyte in CNS. To resolve myelination of MN-SC coculture model with optogenetic stimulation, further studies are needed taking into consideration the timing of optogenetic stimulation, premyelination stage and/or myelinating stage, and frequency of stimulation, similar to impulse activity of MNs.

However, In any rate, it seems clear that the beneficial effect of CoQ10 during early-stage myelination process, which was previously reported in 2-D MN-SC coculture model by Hyung *et al.,*[45] was still realized in the present 3-D MN-SC coculture model.

2. Conclusion

In this dissertation, we presented a simple and reproducible 2-D and 3-D MN-SC coculture models to study the axon growth and myelination process of MNs in the presence of SCs. First, using a 2-D coculture of MNs and SCs, we found that SC plays a vital role in providing proper environment for the biological fate of MN, such as cellular viability, axon growth, and myelination. We also found that PGRN secreted by SCs could be a potential neurotrophic factor for MNs for improving the viability and axon growth of MN. In addition, we reported that optogenetic stimulation alone could improve the axon outgrowth of MNs in the absence of SCs. We also presented that Co-Q10 can be used to accelerate myelination process of MN in the presence of SCs. We finally presented a microfluidic biochip model as a 3-D MN-SC coculture platform to mimic 3-D microenvironment for axon development and myelination of MN.

In conclusion, *in vitro* 2-D and 3-D MN-SC coculture models presented in this dissertation help us to understand the interactions between MNs and SCs in terms of axon regeneration and myelination of MN. We believe that these models can be used in the future as an *ex vivo* tool to understand the mechanisms of motor neuron diseases such as amyotrophic lateral sclerosis (ALS) as well as of repair of damaged motor neurons.

References

[1] Bartzokis G, Lu PH, Mintz J. Human brain myelination and amyloid beta deposition in Alzheimer's disease. Alzheimers Dement 2007;3:122-5.

[2] Baumann N, Pham-Dinh D. Biology of oligodendrocyte and myelin in the mammalian central nervous system. Physiol Rev 2001;81, 871-927.

[3] Jessen KR and Mirsky R. Negative regulation of myelination: relevance for development, injury, and demyelinating disease. Glia 2008;56:1552-65.

[4] Sereda MW, Meyer zu Horste G, Suter U, Uzma N, Nave KA. Therapeutic administration of progesterone antagonist in a model of Charcot-Marie-Tooth disease (CMT-1A). Nat Med 2003;9:1533-37.

[5] Pabari A, Lloyd-Hughes H, Seifalian AM and Mosahebi A. Nerve conduits for peripheral nerve surgery. Plast Reconstr Surg 2014;133:1420-30.

[6] Whitlock EL, Tuffaha SH, Luciano JP, Yan Y, Hunter DA, Magill CK et al. Processed allografts and type I collagen conduits for repair of peripheral nerve gaps. Muscle Nerve 2009;39:787-99.

[7] Ray WZ and Mackinnon SE. Management of nerve gaps: autografts, allografts, nerve transfers, and end-to-side neurorrhaphy. Exp Neurol 2010;223:77-85.

[8] Zhang Y, Luo H, Zhang Z, Lu Y, Huang X, Yang L et al. A nerve graft constructed with xenogeneic acellular nerve matrix and autologous adipose-derived mesenchymal stem cells. Biomaterials 2010;31: 5312-24.

[9] Xu X, Yee WC, Hwang PY, Yu H, Wan AC, Gao S et al. Peripheral nerve regeneration with sustained release of poly(phosphoester) microencapsulated nerve growth factor within nerve guide conduits. Biomaterials 2003;24:2405-12.

[10] Alluin O, Wittmann C, Marqueste T, Chabas JF, Garcia S, Lavaut MN et al. Functional recovery after peripheral nerve injury and implantation of a collagen guide. Biomaterials 2009;30:363-73.

[11] Huang W, Begum R, Barber T, Ibba V, Tee NC, Hussain M et al. Regenerative potential of silk conduits in repair of peripheral nerve injury in adult rats. Biomaterials 2012;33:59-71.

[12] Honkanen H, Lahti O, Nissinen M, Myllyla RM, Kangas S, Paivalainen S et al. Isolation, purification and expansion of myelination-competent, neonatal mouse Schwann cells. Eur J Neurosci 2007;26:953-64.

[13] Paivalainen S, Nissinen M, Honkanen H, Lahti O, Kangas SM, Peltonen J et al. Myelination in mouse dorsal root ganglion/Schwann cell cocultures. Mol Cell Neurosci 2008;37:568-78.

[14] Taylor AM, Blurton-Jones M, Rhee SW, Cribbs DH, Cotman CW, Jeon NL. A microfluidic culture platform for CNS axonal injury, regeneration and transport. Nat Methods 2005;2:599-605.

[15] Watkins TA, Emery B, Mulinyawe S, Barres BA. Distinct stages of myelination regulated by gamma-secretase and astrocytes in a rapidly myelinating CNS coculture system. Neuron 2008;60:555-69.

[16] Gingras M, Beaulieu MM, Gagnon V, Durham HD, Berthod F. In vitro study of axonal migration and myelination of motor neurons in a three-dimensional tissue-engineered model. Glia 2008;56:354-64.

[17] Haastert K, Grosskreutz J, Jaeckel M, Laderer C, Bufler J, Grothe C et al. Rat embryonic motoneurons in long-term co-culture with Schwann cells--a system to investigate motoneuron diseases on a cellular level in vitro. J Neurosci Methods 2005;142:275-84.

[18] Wheeler AR, Throndset WR, Whelan RJ, Leach AM, Zare RN, Liao YH et al. Microfluidic device for single-cell analysis. Anal Chem 2003;75:3581-6.

[19] Park JW, Vahidi B, Taylor AM, Rhee SW, Jeon NL. Microfluidic culture platform for neuroscience research. Nat Protoc 2006;1:2128-36.

[20] Park J, Koito H, Li J, Han A. Microfluidic compartmentalized co-culture platform for CNS axon myelination research. Biomed Microdevices 2009;11:1145-53.

[21] Park J, Koito H, Li J and Han A. Multi-compartment neuron-glia co-culture platform for localized CNS axon-glia interaction study. Lab Chip 2012;12: 3296-3304.

[22] Bang S, Na S, Jang JM, Kim J, Jeon NL. Engineering-Aligned 3D Neural Circuit in Microfluidic Device. Adv Healthc Mater 2016;5:159-166.

[23] Acheson A, Barker PA, Alderson RF, Miller FD, Murphy RA. Detection of brain-derived neurotrophic factor-like activity in fibroblasts and Schwann cells: inhibition by antibodies to NGF. Neuron 1991;7:265-75.

[24] Frostick SP, Yin Q, Kemp GJ. Schwann cells, neurotrophic factors, and peripheral nerve regeneration. Microsurgery 1998;18:397-405.

[25] Airaksinen MS, Saarma M. The GDNF family: signalling, biological functions and therapeutic value. Nat Rev Neurosci 2002;3:383-94.

[26] Friedman B, Scherer SS, Rudge JS, Helgren M, Morrisey D, McClain J et al. Regulation of ciliary neurotrophic factor expression in myelin-related Schwann cells in vivo. Neuron 1992;9:295-305.

[27] Ozdinler PH, Macklis JD. IGF-I specifically enhances axon outgrowth of corticospinal motor neurons. Nat Neurosci 2006;9:1371-81.

[28] Sosa L, Dupraz S, Laurino L, Bollati F, Bisbal M, Caceres A et al. IGF-1 receptor is essential for the establishment of hippocampal neuronal polarity. Nat Neurosci 2006;9:993-5.

[29] Nguyen AD, Nguyen TA, Martens LH, Mitic LL, Farese RV. Progranulin: at the interface of neurodegenerative and metabolic diseases. Trends Endocrinol Metab 2013;24,597-606.

[30] Hu F, Padukkavidana T, Vaegter CB, Brady OA, Zheng Y, Mackenzie IR et al. Sortilin-mediated endocytosis determines levels of the frontotemporal dementia protein, progranulin. Neuron 2010;68:654-67.

[31] Gao X, Joselin AP, Wang L, Kar A, Ray P, Bateman A et al. Progranulin promotes neurite outgrowth and neuronal

differentiation by regulating GSK-3beta. Protein Cell 2010;1:552-62.

[32] He Z, Ong CH, Halper J, Bateman A. Progranulin is a mediator of the wound response. Nat Med 2003;9:225-9.

[33] Eguchi R, Nakano T, Wakabayashi I. Progranulin and granulin-like protein as novel VEGF-independent angiogenic factors derived from human mesothelioma cells. Oncogene 2016;doi:10.1038.

[34] Gass J, Lee WC, Cook C, Finch N, Stetler C, Jansen-West K et al. Progranulin regulates neuronal outgrowth independent of sortilin. Mol Neurodegener 2012;7:33.

[35] Ryan CL, Baranowski DC, Chitramuthu BP, Malik S, Li Z, Cao M et al. Progranulin is expressed within motor neurons and promotes neuronal cell survival. BMC Neurosci 2009;10:130.

[36] Al-Majed AA, Tam SL, Gordon T. Electrical stimulation accelerates and enhances expression of regeneration-associated genes in regenerating rat femoral motoneurons. Cell Mol Neurobiol 2004;24:379-402.

[37] Brushart TM, Hoffman PN, Royall RM, Murinson BB, Witzel C, Gordon T. Electrical stimulation promotes motoneuron regeneration without increasing its speed or conditioning the neuron. J Neurosci 2002;22:6631-8.

[38] Singh B, Xu QG, Franz CK, Zhang R, Dalton C, Gordon T et al. Accelerated axon outgrowth, guidance, and target reinnervation across nerve transection gaps following a brief electrical stimulation paradigm. J Neurosurg 2012;116:498-512.

[39] Demerens C, Stankoff B, Logak M, Anglade P, Allinquant B, Couraud F et al. Induction of myelination in the central nervous system by electrical activity. Proc Natl Acad Sci U S A 1996;93:9887-92.

[40] Gunaydin LA, Yizhar O, Berndt A, Sohal VS, Deisseroth K, Hegemann P. Ultrafast optogenetic control. Nat Neurosci 2010;13:387-92.

[41] Haubensak W, Kunwar PS, Cai H, Ciocchi S, Wall NR, Ponnusamy R et al. Genetic dissection of an amygdala microcircuit that gates conditioned fear. Nature 2010;468;270-6.

[42] Witten IB, Lin SC, Brodsky M, Prakash R, Diester I, Anikeeva P et al. Cholinergic interneurons control local circuit activity and cocaine conditioning. Science 2010;330:1677-81.

[43] Lin JY, Knutsen PM, Muller A, Kleinfeld D, Tsien RY. ReaChR: a red-shifted variant of channelrhodopsin enables

deep transcranial optogenetic excitation. Nat Neurosci 2013;16:1499-508.

[44] Park S, Koppes RA, Froriep UP, Jia X, Achyuta AK, McLaughlin BL et al. Optogenetic control of nerve growth. Sci Rep 2015;5:9669.

[45] Hyung S, Yoon Lee B, Park JC, Kim J, Hur EM, Francis Suh JK. Coculture of Primary Motor Neurons and Schwann Cells as a Model for In Vitro Myelination. Sci Rep 2015;5:15122.

[46] Shaw PJ, Eggett CJ. Molecular factors underlying selective vulnerability of motor neurons to neurodegeneration in amyotrophic lateral sclerosis. J Neurol 2000;247: Suppl 1, I17-2.

[47] Wiese S, Herrmann T, Drepper C, Jablonka S, Funk N, Klausmeyer A et al. Isolation and enrichment of embryonic mouse motoneurons from the lumbar spinal cord of individual mouse embryos. Nat Protoc 2010;5:31-8.

[48] Pereira JA, Lebrun-Julien F, Suter U. Molecular mechanisms regulating myelination in the peripheral nervous system. Trends Neurosci 2012;35:123-34.

[49] Decker L, Desmarquet-Trin-Dinh C, Taillebourg E, Ghislain J, Vallat JM, Charnay P. Peripheral myelin

maintenance is a dynamic process requiring constant Krox20 expression. J Neurosci 2006;26:9771-9.

[50] Topilko P, Schneider-Maunoury S, Levi G, Baron-Van Evercooren A, Chennoufi AB, Seitanidou T et al. Krox-20 controls myelination in the peripheral nervous system. Nature 1994;371:796-9.

[51] Emery B. Regulation of oligodendrocyte differentiation and myelination. Science 2010;330:779-82.

[52] Bensimon G, Lacomblez L, Meininger V. A controlled trial of riluzole in amyotrophic lateral sclerosis. ALS/Riluzole Study Group. N Engl J Med 1994;330:585-9.

[53] Ferrante RJ, Andreassen OA, Dedeoglu A, Ferrante KL, Jenkins BG, Hersch SM et al. Therapeutic effects of coenzyme Q10 and remacemide in transgenic mouse models of Huntington's disease. J Neurosci 2002;22:1592-9.

[54] Matthews RT, Yang L, Browne S, Baik M, Beal MF. Coenzyme Q10 administration increases brain mitochondrial concentrations and exerts neuroprotective effects. Proc Natl Acad Sci U S A 1998;95:8892-7.

[55] Jessen KR, Mirsky R. The origin and development of glial cells in peripheral nerves. Nat Rev Neurosci 2005;6:671-82.

[56] Henderson CE, Phillips HS, Pollock RA, Davies AM, Lemeulle C, Armanini M et al. GDNF: a potent survival factor for motoneurons present in peripheral nerve and muscle. Science 1994;266:1062-4.

[57] Hammarberg H, Piehl F, Cullheim S, Fjell J, Hokfelt T and Fried K. GDNF mRNA in Schwann cells and DRG satellite cells after chronic sciatic nerve injury. Neuroreport 1996;7:857-60.

[58] Lin G, Zhang H, Sun F, Lu Z, Reed-Maldonado A, Lee YC et al. Brain-derived neurotrophic factor promotes nerve regeneration by activating the JAK/STAT pathway in Schwann cells. Transl Androl Urol 2016;5:167-75.

[59] Sendtner M, Kreutzberg GW, Thoenen H. Ciliary neurotrophic factor prevents the degeneration of motor neurons after axotomy. Nature 1990;345: 440-1.

[60] Huh D, Kim HJ, Fraser JP, Shea DE, Khan M, Bahinski A et al. Microfabrication of human organs-on-chips. Nat Protoc 2013;8:2135-57.

[61] Shin J, Kim G, Kabir MH, Park SJ, Lee ST, Lee C. Use of composite protein database including search result sequences for mass spectrometric analysis of cell secretome. PLoS One 2015;10:e0121692.

[62] Jiang M, Chen G. High Ca2+-phosphate transfection efficiency in low-density neuronal cultures. Nat Protoc 2006;1:695-700.

[63] Zhu J, Nathan C, Jin W, Sim D, Ashcroft GS, Wahl SM et al. Conversion of proepithelin to epithelins: roles of SLPI and elastase in host defense and wound repair. Cell 2002;111:867-78.

[64] Gordon T, Udina E, Verge VM, de Chaves EI. Brief electrical stimulation accelerates axon regeneration in the peripheral nervous system and promotes sensory axon regeneration in the central nervous system. Motor Control 2009;13:412-41.

[65] McCaig CD, Rajnicek AM. Electrical fields, nerve growth and nerve regeneration. Exp Physiol 1991;76:473-94.

[66] Thompson DM, Koppes AN, Hardy JG, Schmidt CE. Electrical stimuli in the central nervous system microenvironment. Annu Rev Biomed Eng 2014;16: 397-430.

[67] Al-Majed AA, Neumann CM, Brushart TM, Gordon T. Brief electrical stimulation promotes the speed and accuracy of motor axonal regeneration. J Neurosci 2000;20:2602-8.

[68] Lu MC, Ho CY, Hsu SF, Lee HC, Lin JH, Yao CH et al. Effects of electrical stimulation at different frequencies on regeneration of transected peripheral nerve. Neurorehabil Neural Repair 2008;22:367-73.

[69] Stevens B, Tanner S, Fields RD. Control of myelination by specific patterns of neural impulses. J Neurosci 18, 9303-9311 (1998).

[70] Koppes AN, Keating KW, McGregor AL, Koppes RA, Kearns KR, Ziemba AM et al. Robust neurite extension following exogenous electrical stimulation within single walled carbon nanotube-composite hydrogels. Acta Biomater 2016;39: 34-43.

[71] Jang JY. Optogenetic stimulation promotes axon outgrowth of motor neuron in vitro: Master's Thesis. Seoul: Ewha womas Univ.; 2016.

[72] Kleinlogel S, Feldbauer K, Dempski RE, Fotis H, Wood PG, Bamann C et al. Ultra light-sensitive and fast neuronal activation with the Ca(2)+-permeable channelrhodopsin CatCh. Nat Neurosci 2011;14:513-18.

[73] Feldbauer K, Zimmermann D, Pintschovius V, Spitz J, Bamann C, Bamberg E. Channelrhodopsin-2 is a leaky proton pump. Proc Natl Acad Sci U S A 2009;106:12317-22.

[74] Szobota S, Gorostiza P, Del Bene F, Wyart C, Fortin DL, Kolstad KD et al. Remote control of neuronal activity with a light-gated glutamate receptor. Neuron 2007;54:535-45.

[75] Bloch-Gallego E, Huchet M, el M'Hamdi H, Xie FK, Tanaka H, Henderson CE. Survival in vitro of motoneurons identified or purified by novel antibody-based methods is selectively enhanced by muscle-derived factors. Development 1991;111:221-32.

[76] Ullian EM, Harris BT, Wu A, Chan JR, Barres BA. Schwann cells and astrocytes induce synapse formation by spinal motor neurons in culture. Mol Cell Neurosci 2004;25:241-51.

[77] Boyden ES, Zhang F, Bamberg E, Nagel G, Deisseroth K. Millisecond-timescale, genetically targeted optical control of neural activity. Nat Neurosci 2005;8:1263-8.

[78] Aglah C, Gordon T, Posse de Chaves EI. cAMP promotes neurite outgrowth and extension through protein kinase A but independently of Erk activation in cultured rat motoneurons. Neuropharmacology 2008;55:8-17.

[79] Chierzi S, Ratto GM, Verma P, Fawcett JW. The ability of axons to regenerate their growth cones depends on axonal type and age, and is regulated by calcium, cAMP and ERK. Eur J Neurosci 2005;21:2051-62.

[80] Hanson MG, Jr., Shen S, Wiemelt AP, McMorris FA and Barres BA. Cyclic AMP elevation is sufficient to promote the survival of spinal motor neurons in vitro. J Neurosci 1998;18:7361-71.

[81] Zhou Z, Tanaka KF, Matsunaga S, Iseki M, Watanabe M, Matsuki N et al. Photoactivated adenylyl cyclase (PAC) reveals novel mechanisms underlying cAMP-dependent axonal morphogenesis. Sci Rep 2016;5:19679.

[82] Uzel SG, Platt RJ, Subramanian V, Pearl TM, Rowlands CJ, Chan V et al. Microfluidic device for the formation of optically excitable, three-dimensional, compartmentalized motor units. Sci Adv 2016;2:e1501429.

[83] Raman R, Cvetkovic C, Uzel SG, Platt RJ, Sengupta P, Kamm RD et al. Optogenetic skeletal muscle-powered adaptive biological machines. Proc Natl Acad Sci U S A 2016;113:3497-502.

[84] Callizot N, Combes M, Steinschneider R, Poindron P. A new long term *in vitro* model of myelination. Exp Cell Res 2011;317:2374-83.

[85] Stettner M, Wolffram K, Mausberg AK, Wolf C, Heikaus S, Derksen A et al. A reliable in vitro model for studying peripheral nerve myelination in mouse. J Neurosci Methods 2013;214:,69-79.

[86] Bahr M, Hopkins JM, Bunge RP. In vitro myelination of regenerating adult rat retinal ganglion cell axons by Schwann cells. Glia 1991;4:529-33.

[87] Taylor AR, Robinson MB, Milligan CE. In vitro methods to prepare astrocyte and motoneuron cultures for the investigation of potential in vivo interactions. Nat. Protocols 2007;2:1499-507.

[88] King AE, Dickson TC, Blizzard CA, Woodhouse A, Foster SS, Chung RS et al. Neuron-glia interactions underlie ALS-like axonal cytoskeletal pathology. Neurobiol Aging 2011;32:459-69.

[89] Meyer zu Horste G, Prukop T, Liebetanz D, Mobius W, Nave KA, Sereda MW. Antiprogesterone therapy uncouples axonal loss from demyelination in a transgenic rat model of CMT1A neuropathy. Ann Neurol 2007;61:61-72.

[90] Viader A, Golden JP, Baloh RH, Schmidt RE, Hunter DA, Milbrandt J. Schwann cell mitochondrial metabolism supports long-term axonal survival and peripheral nerve function. J Neurosci 2011;31:10128-40.

[91] Reddy LV, Koirala S, Sugiura Y, Herrera AA, Ko CP. Glial cells maintain synaptic structure and function and promote development of the neuromuscular junction in vivo. Neuron 2003;40:563-80.

[92] Scheib J and Hoke A. Advances in peripheral nerve regeneration. Nat Rev Neurol 2013;9:668-76.

[93] Son YJ and Thompson WJ. Schwann cell processes guide regeneration of peripheral axons. Neuron 1995;14:125-32.

[94] Woodhoo A, Alonso MB, Droggiti A, Turmaine M, D'Antonio M, Parkinson DB et al. Notch controls embryonic Schwann cell differentiation, postnatal myelination and adult plasticity. Nat Neurosci 2009;12:839-47.

[95] Buraschi S, Xu SQ, Stefanello M, Moskalev I, Morcavallo A, Genua M et al. Suppression of progranulin expression inhibits bladder cancer growth and sensitizes cancer cells to cisplatin. Oncotarget 2016; doi:10.18632.

[96] Feneberg E, Steinacker P, Volk AE, Weishaupt JH, Wollmer MA, Boxer A et al. Progranulin as a candidate biomarker for therapeutic trial in patients with ALS and FTLD. J Neural Transm (Vienna) 2016;123:289-96.

[97] Kuse Y, Tsuruma K, Sugitani S, Izawa H, Ohno Y, Shimazawa M et al. Progranulin promotes the retinal precursor cell proliferation and the photoreceptor differentiation in the mouse retina. Sci Rep 2016;6:23811.

[98] Brennan BP, Hudson JI, Jensen JE, McCarthy J, Roberts JL, Prescot AP et al. Rapid enhancement of glutamatergic

neurotransmission in bipolar depression following treatment with riluzole. Neuropsychopharmacology 2010;35:834-46.

[99] Galer BS, Twilling LL, Harle J, Cluff RS, Friedman E, Rowbotham MC. Lack of efficacy of riluzole in the treatment of peripheral neuropathic pain conditions. Neurology 2000;55:971-5.

[100] Bhagavan HN and Chopra RK. Coenzyme Q10: absorption, tissue uptake, metabolism and pharmacokinetics. Free Radic Res 2006;40:445-53.

[101] Favit A, Nicoletti F, Scapagnini U and Canonico PL. Ubiquinone protects cultured neurons against spontaneous and excitotoxin-induced degeneration. J Cereb Blood Flow Metab 1992;12:638-45.

[102] McCarthy S, Somayajulu M, Sikorska M, Borowy-Borowski H, Pandey S. Paraquat induces oxidative stress and neuronal cell death; neuroprotection by water-soluble Coenzyme Q10. Toxicol Appl Pharmacol 2004;201:21-31.

[103] Zalc B and Fields RD. Do Action Potentials Regulate Myelination? Neuroscientist 2000;6:5-13.

Acknowledgements

This research was supported by National Agenda Project of Korea National Research Council of Science & Technology (NAP-09-04 to JKFS), Institutional Grant from KIST (2N38341 to JKFS). The authors would like to thank Su Sung Kim for the TEM preparation. Plasmid of CatCh-EYFP was constructed and provided by Dr. Eun Mi Hwang of Center for Functional Connectomes of Korea Institute of Science and Technology. Confocal microscopy imaging was carried out on Carl Zeiss microscopy at the Yonsei Advanced Imaging Center, Yonsei University College of Medicine.

Abstract (in korean)

운동신경과 슈반세포 공동 배양 모델에서의 축삭 성장과 수초 형성

<지도교수 박종철>

연세대대학교 대학원 의과학과

형수진

신경시스템에서 수초의 형성은 축삭 주위를 둘러싸고 있는 중요한 구조로 수초형성에 의해 빠른 신경도약을 가능하게 하는 절연체이다. 중추신경계에서는 희돌기신경교, 말초신경계에서는 슈반세포가 축삭 주위를 감싸는데, 중추신경계의 희돌기신경교는 세포질을 이용하여 여러 신경세포의 축삭을 둘러쌓는 반면, 말초신경계의 슈반세포는 세포체 전체가 하나의 슈반세포가 하나의 신경세포 축삭의 일부분을 감싸고 있는 차이가 있다. 이러한

신경계에서 손상을 받으면 지금까지는 중추신경계에서는 재생이 불가능하고 말초신경계에서는 손상 후 재생이 이루어 진다고 보고 되어 왔지만 이러한 말초신경계의 재생도 환자의 나이, 손상의 정도, 재생의 환경에 의해 크게 좌우된다. 많은 문헌에서는 손상모델 뿐만 아니라 질환모델에서 신경재생을 위한 연구를 진행하고 있지만 아직까지 명확하게 해결책을 찾지 못했고, 여러가지 재생의 한계점을 풀지 못했다. 이 논문에서는 이러한 한계점을 극복하기 위해 신경계 중 움직임을 조절하는 운동신경계의 이차원적과 삼차원적인 *in vitro* 모델을 확립하고 여기에 축삭의 성장과 수초형성을 촉진시키는 요인을 연구하고자 한다. 먼저, 이차원적 운동신경모델의 형성으로 운동신경과 슈반세포의 상호작용을 이해하고 그 다음 microfluidic 바이오칩을 이용하여 삼차원적인 in vitro 모델 형성으로 in vivo 와 유사한 환경을 재현하였다. 지금까지 알려진 운동신경은 배양했을 때 일주일 이상 그 생존율을 지속하기 어렵다. 하지만 슈반세포와의 공동배양을 통해 운동신경의 생존율은 한 달간 지속 되었다. 이 기간 동안 슈반세포는 운동신경의 생존 뿐만 아니라 축삭의 성장까지 증가시켰다. 이러한 슈반세포의 효과는 슈반세포에서 분비하는 7.5 개의 granulins (GRN)로 이루어진 Progranulin (PGRN)이라는 단백질에 의해서 조절되고

그 중 GRN C 와 E 가 강력한 neurotrophic 요소로서 슈반세포가 없는 상태에서 운동신경세포의 생존을 이주 이상 지속시켰다. 또한 우리는 광유전자를 이용하여 운동신경 축삭의 성장을 촉진시키는데 그 방법을 확립하였다. 게다가 슈반세포는 수초를 형성하는 중요한 세포로서 이 논문에서는 슈반세포의 수초형성 과정을 정량적으로 측정하였고 이 공동배양 모델을 통해 coenzyme Q10 이 수초형성을 촉진시키는 약물인 점을 확인 할 수 있었다. 이러한 공동배양 모델은 앞에서 언급한 운동신경 재생의 한계점을 극복하는데 중요한 도구로 사용 될 수 있다. 또한 수초형성 메카니즘을 분석하고고 ALS 와 같은 운동신경 질환을 연구하는데 약물 스크리닝을 할 수 있는 도구로서도 도움을 준다. 그 뿐만 아니라 *in vivo* 모사 *in vitro* 모델은, 손상 후 재생의 한계점을 밝혀혀 세포간의 정밀한 메카니즘을 연구하는데 용이하다.

핵심되는 말: 운동신경, 슈반세포, 축삭 성장, 수초 형성, progranulin, 광유전자 자극, 삼차원적 microfluidic 바이오칩